F-AM-A1 SCANNING ELECTRON MICROSCOPIC STUDIES OF FELINE HEARTS; ENDOCARDIAL AND MYOCARDIAL STRUCTURES. S.H. Song, Department of Biophysics, Faculty of Medicine, University of Western Ontario, London, Ontario, Canada.

Although the ultrastructure of mammalian cardiac tissues has been studied in detail with light or transmission electron microscopes, surface characteristics of endocardial and myocardial fibers are seldom investigated. We used the scanning electron microscope (SEM) to observe more clearly the surface structures inside the heart. The specimen was prepared with a camphene dry method, using several small pieces cut from the interventricular septum and the left and right ventricular and auricular walls. Many apertures were observed between the papillary muscles and the trabeculae carneæ. This suggested possible communication between coronary vessels and the ventricular lumen. With high magnifications (5,000 to 20,000X) three distinct structures were observed. Granulated endothelial cells of about 0.5 μm length and diameter covered the endocardium. There were also two types of cross bands elevated from the surface of the myofibrils. Larger bands were regularly arranged with a spacing of approximately 4-5 μm. Small bands were seen between these. These surface structures observed with the SEM seem more realistic in three dimensions than the Z lines and H bands in the sarcomere described from transmission microscopes. The functional implications of the sarcomere unit in relation to myocardial contractility will be discussed.

S.H. Song is a Senior Research Fellow of Ontario Heart Foundation. This project is supported by an Ontario Heart Foundation Research Grant.

F-AM-A2 VISUALIZATION OF DENSE BODIES IN SMOOTH MUSCLE BY LIGHT MICROSCOPY. Keith E. Summers, Joan A. Moses*, and Robert V. Rice, Department of Biological Sciences, Carnegie-Mellon University, Pittsburgh, Pennsylvania 15213.

Dense bodies in living smooth muscle of cow stomach (Pilae ruminis) were visualized by Nomarski light microscopy in resting, contracted, and relaxed states. The same muscle tissue used for light microscopy was fixed and embedded; electron microscopy of serial sections of such specimens confirmed the light microscopy identification of dense bodies. These findings confirm the general acceptance of dense bodies as an important organelle in smooth muscle cells and refute a recent speculation that dense bodies are artifacts of electron microscopical fixation methods. The results show that dense bodies are not of uniform length but vary from less than 2 microns to more than 10 microns. Other studies indicate that dense bodies are composed of 10 nm filaments and amorphous protein. These filaments have a principal protein component which has been named mesosin.

F-AM-A3 THE T-SYSTEMS AND STRIATIONS OF FROG SKELETAL MUSCLE ARE SPIRAL. Lee D. Peachey and Brenda R. Eisenberg,* Department of Biology, University of Pennsylvania, Philadelphia, Pennsylvania 19174 and Department of Medicine, U.C.L.A. Medical School, Los Angeles, California 90024 (Intr. by Robert S. Eisenberg).

We always have thought that the striations of striated muscle are descrete units, lying in planes roughly transverse to the fiber axis. According to this, each T-system is also descrete and separated from longitudinally adjacent T-systems, except for occasional longitudinal extensions of tubules alongside myofibrils. We have attempted to reconstruct one complete T-system from a series of 1000 kV transmission electron micrographs of serial 0.5-1.0 μm thick slices cut transversely from frog skeletal muscles soaked in exogenous peroxidase and stained with DAB-H_2O_2-Os. This reconstruction was found to be impossible because one presumed separate T-system was found to be continuous in a spiral manner with the two adjacent T-systems in the longitudinal direction. The ramp-like connections observed repeated for at least three sarcomeres so far reconstructed in five fibers examined, suggesting that a spiral arrangement of the T-system is common in these fibers. Since the T-system in frog twitch fibers is rather precisely localized at the Z-lines of the fibrils, and since the T-system is spiral, it follows that the muscle bands must also be spirally arranged. These connections are alongside longitudinal dislocations in the striations of adjacent myofibrils, as would be required in a spiral arrangement of bands. These dislocations probably correspond to vernier formations seen in longitudinal sections. The spiral arrangement of bands has been reported twice before, first by van Leeuenhoek in 1718, but the discovery seems to have been lost as often as made. (Supported by N.I.H. Grants RR-592 and HL-15835, and a M.D.A.A. Grant).

F-AM-A4 HIGH VOLTAGE ELECTRON MICROSCOPY OF SARCOPLASMIC RETICULUM IN FROG SKELETAL MUSCLE. Craig H. Bailey* and Lee D. Peachey, Department of Biology, University of Pennsylvania, Philadelphia, Pennsylvania 19174.

Our knowledge of the structure of the sarcoplasmic reticulum (SR) in frog twitch muscle fibers comes from the study of thin (approx. 0.1 μm) sections of embedded tissue by transmission electron microscopy. Only a small portion of the SR associated with one myofibril is contained in the thickness of the section, and the complete three-dimensional nature of the SR must be inferred from a collection of such images from different planes and with different orientations. Using high voltage electron microscopy (HVEM), one can examine slices of embedded tissue 1 μm or more in thickness. With a highly selective stain for the SR(DAB-H_2O_2 and Os-ferrocyanide) and HVEM, we have been able to visualize very large expanses of SR in slices from 0.25 to 1.0 μm in thickness without excessive interference in the images from myofibrils lying above or below the SR in the thickness of the slice. The electron microscope accelerating voltage used was 1000 kV. Longitudinal thick slices viewed in stereo resemble earlier artist's reconstructions and confirm many of the morphological specializations and three-dimensional relationships of the SR previously worked out from thin sections. The combination of highly selective staining and HVEM stereoscopy of thick slices provides a realistic approach to the otherwise difficult task of describing accurately the full three-dimensional extent and form of a complex organelle such as the SR, and should prove to be useful in aiding a more complete description of this organelle's geometry in other muscle fiber types. (Supported by N.I.H. Grants RR-592 and HL-15835, and by a M.D.A.A. Grant and Postdoctoral Fellowship).

F-AM-A5 QUANTITATIVE MORPHOLOGICAL ANALYSIS OF FROG SKELETAL MUSCLE USING METHODS OF STEREOLOGY.

B. A. Mobley and B. R. Eisenberg*, Departments of Physiology and Medicine, School of Medicine, University of California at Los Angeles, Los Angeles, California 90024.

Stereological techniques of point and intersection counting were used to measure morphological parameters from light and electron micrographs of frog skeletal muscle. Results for sartorius muscle are as follows: myofibrils comprise 83% of fiber volume; their surface to volume ratio is $3.8\mu^{-1}$. Mitochondria comprise 1.6% of fiber volume. Transverse tubules comprise 0.32% of fiber volume, and their surface area per volume of fiber is $0.22\mu^{-1}$. Terminal cisternae of the sarcoplasmic reticulum comprise 4.1% of fiber volume; their surface area per volume of fiber is $0.54\mu^{-1}$. Longitudinal sarcoplasmic reticulum comprises 5.0% of fiber volume, and its surface area per volume of fiber is $1.48\mu^{-1}$. Longitudinal bridges between terminal cisternae on either side of a Z disc were observed infrequently; they make up only 0.035% of fiber volume and their surface area per volume of fiber is $0.009\mu^{-1}$. T-SR junction occurs over 67% of the surface of transverse tubules and over 27% of the surface of terminal cisternae. The surface to volume ratio of the caveolae is $48\mu^{-1}$; caveolae may increase the sarcolemmal surface area by 47%. Essentially the same results were obtained from semitendinosus fibers.

F-AM-A6 ISOLATION OF TRANSVERSE TUBULE VESICLES FROM RABBIT SKELETAL MUSCLE.

A.H. Caswell*, R.J. Baerwald* and J.P. Brunschwig*, Intr. by W.R. Loewenstein, Department of Pharmacology, University of Miami School of Medicine, Miami, Florida 33152

Fluorescence staining and freeze fracture electron microscopy have been employed in isolation and identification of transverse (T) tubule vesicles from skeletal muscle. The intact muscle has been treated with the covalent label, fluorescein isothiocyanate (FSNC). This label stains external membranes including T tubules and plasma membrane. The muscle has been homogenized and fractionated by differential and density gradient centrifugation. A region of high specific activity of FSNC occurs at 22% sucrose in the density gradient from the microsomal fraction. Three morphologically unique vesicle preparations have been identified from freeze fracture of fractions of the muscle homogenate by comparing them with intact membranes. 1. Pure sarcoplasmic reticulum with high density of particles on concave face and few on convex face. 2. Large vesicles of plasma membrane identified by orthogonal shaped particle arrays on A face and indentations of caveolae. 3. The fluorescence labelled preparation having few particles on either face. Since the T tubules and plasma membrane have different and characteristic particle distribution on the fracture faces, electron microscopy of the freeze fractured vesicles allows identification of the FSNC stained fraction as being of T tubule origin. The enzyme profile of the T tubule fraction has been investigated. A Mg-EGTA ATPase but not a Na-K ATPase have been found. Supported by grants NIH 1PO1HL16117, 5 RO1 HL15645, 5KO4 HL70151.

F-AM-A7 TETRODOTOXIN (TTX) BINDING IN NORMAL AND 'DETUBULATED' FROG SARTORIUS MUSCLE. E. Jaimovich*, R.A. Venosa*, P.Shrager and P. Horowicz. Dept. of Physiology, University of Rochester Rochester, New York 14642.

TTX binding, using a bioassay technique, was compared with physiological effects in normal and 'detubulated' muscles for TTX concentrations in the range 0 to 150 nM. 'Detubulation' was produced by soaking muscles in Ringer + 400 mM glycerol for 75 min and then returning to Ringer. The maximum rate of rise of the action potential (V_{max}) and twitch tension were recorded. V_{max} was reduced by one half at about 6-9 nM in both cases. In normal muscle the twitch was reduced by half at 7-9 nM. In both normal and 'detubulated' muscles TTX binding saturates at high TTX concentrations. The maximum binding of TTX was about 36 pmole/g wet wt in normal muscles and 16 pmole/g wet wt in 'detubulated' muscles. Control experiments indicate that neither fiber damage alone nor incubation in glycerol with small stepwise return to Ringer (allowing twitch maintenance) produces any reduction in TTX binding. These results suggest that at least half of the total bound TTX molecules in normal muscle depend on the presence of an intact transverse tubular system.
(Supported by USPHS Grant Nos. 5-PO1-NS10981 and 5-RO1-NS10500)

F-AM-A8 THE EFFECTS OF RUTHENIUM RED ON ELECTRICAL PARAMETERS OF FROG SARTORIUS MUSCLE. J.N. Howell and K.W. Snowdowne*,Departments of Physiology and Pharmacology, Schools of Medicine and Pharmacy, University of Pittsburgh, Pittsburgh, Pa. 15261.

Ruthenium red (RR) (5-25μM), recrystallized from ½ M NH_4OH and dissolved in Hepes Ringer, has little or no effect on resting potentials, input resistance and action potential overshoots over a four hour exposure period. However, these concentrations have dose-dependent effects on action potential thresholds (t), rates of rise (rr) and rates of repolarization (rp). At 25μM, RR alters t from about-50 mV to -20 mV and reduces the rr by 70%. The effects are maximal within five minutes. Only the effect on t is reversible following a 30 minute exposure to RR. The effect on the rp is slower to develop and the rate of development is concentration dependent. The maximum reduction in rp, 70%, was observed following a four hour exposure to 25μM RR. Fibers exposed to concentrations of RR>50μM exhibit declining resting potentials and membrane resistance and, ultimately, retraction clots.

Although the initial effects of RR in theμmolar range are similar to the effects of calcium in concentrations > 2 mM, preliminary results of substitution experiments suggest that the presence of 50μM RR cannot prevent the membrane changes that result from the withdrawal of calcium. Thus it seems likely that calcium at low concentrations interacts with sites having little affinity for RR, whereas calcium at high concentrations interacts with sites having high affinity for RR. The time course of the RR effect on rp is consistent with the hypothesis that the membrane is slightly permeable to RR and that this effect is mediated by intracellular RR.

F-AM-A9 Contractile Impulse Conduction in the Embryonic Heart. C.E. Challice and S. Virágh*± Department of Physics, University of Calgary, Calgary, Alberta T2N 1N4, Canada.

As part of a study of the development of the atrio-ventricular (A-V) conduction system in the heart of the mouse it has been found that at 12 days of embryonic life a structure has appeared in the dorsal wall of the A-V canal which links the atrial muscle with the ventricular trabeculae. This structure, designated the A-V ribbon, appears to give rise to the anlage of the A-V node and the His bundle a day or so later. However, until the invasion of the connective tissue separating atria and ventricles(which ultimately becomes the annulus fibrosus) there remains muscular continuity along the ventral wall of the A-V canal, providing a pathway to the atrio-bulbar junction which is geometrically shorter than that to the farther parts of the primitive ventricular chambers. Even so, there is a clear and well defined sequence of contraction of sinus node-atrium-ventricles-bulbus. The contractile impulse has not been observed to cause contraction in the bulbus before the ventricles despite the shorter pathway, in which no evidence of muscular discontinuity has been found. Attempts have been made to account for this observation. It seems possible, despite the physical contact at the atrio-bulbar junction, which occurs during the twisting process in the heart's embryonic development, that functional electrical transmission is not established at this point. On the other hand it seems possible also that there may be an electromechanical ingredient in the mechanism of maintenance of the contractile sequence (cf. Pollack, J. Electrocardiology 7, 245, 1974). At the present time the emperimental evidence does not permit conclusive discrimination between the possibilities.

±Permanent address, Postgraduate Medical School, Budapest, Hungary.

F-AM-A10 ALTERNATING CURRENT ANALYSIS IN SCORPION MUSCLE FIBERS Arieh Gilai (intr. by S. Nakajima), Hebrew University, Jerusalem, Israel

Scorpion muscle fibers are tubular, having a central sarcoplasmic core. The myofibrils are lamellated and symmetrically arranged around the core. The transverse tubules (TT) are open to the extracellular medium, each TT can be traced from the surface membrane down to the cell core. The radial symmetrical arrangement of the TT system in a cross section, enables one to derive values for electrical components of one TT by treating the TT as a core conductor rather than a complex network. Since a striated muscle fiber is composed of many identical repetitive sarcomeres, the lumped constant transmission line theory approximates the distributed electrical properties of one sarcomere with an error of about 0.1%. These properties were completely characterized and analyzed by measuring two independent functions of frequency, i.e., the characteristic impedance and the propagation function. The impedance of a single tubular muscle fiber was determined with microelectrodes over the frequency range 1 Hz. to 1.5 k Hz. The results were fitted to a possible equivalent circuit model which is based on morphological evidence. The average component values for this model are: R_i=209 ohm cm, R_m & R_T=980 ohm cm^2 (referred to unit area of surface and TT membrane), C_m & C_T=0.9 μF/cm^2 and R_L=103 ohm cm. Relating the equivalent circuit to ultrastructure shows that the average component values are consistent with the hypothesis that the TT is open to the extracellular medium, the electrical capacity of surface and TT membranes is about 1 μF/cm^2, and the spread of surface depolarization into the TT is attenuated by about 25%.

F-AM-A11 DECIPHERING NONLINEAR MEMBRANES: DISTORTION FROM CABLE LENGTH. J. M. Kootsey, J. Vereecke, N. Shigeto, M. Lieberman, and E. A. Johnson, Department of Physiology, Duke University Medical Center, Durham, North Carolina 27710.

The task of deciphering membrane characteristics from input measurements on a cylindrical cell is especially difficult when the membrane is nonlinear. This problem arises from variations in membrane state along the length of the cylinder and would vanish if it were made sufficiently short. Although evident in principle from cable theory, this dependence of input characteristics on length has never been clearly demonstrated by calculation and experiment. In the work described, the different input characteristics for long and short synthetic strands of cardiac muscle were closely matched by the different input characteristics of long and short theoretical cables with identical membrane properties. These input characteristics included not only the steady-state current voltage relationships, but also the time course of displacement in membrane potential after momentary voltage clamp at a point during repolarization of an action potential. Long cables showed qualitative features not present in the membrane description, such as an unexpected inward current. The input characteristics approached the membrane characteristics for fiber lengths less than 1/5 of the resting DC length constant. (Supported, in part, by grants from the National Institutes of Health, HL 12157 and HL 11307, and by American Heart Association grant 71160.)

F-AM-A12 ANALYSIS OF THE THREE-MICROELECTRODE METHOD AS APPLIED TO INWARD CURRENTS IN CARDIAC PURKINJE FIBERS. R.S. Kass and R.W. Tsien, Department of Physiology, Yale School of Medicine, New Haven, Connecticut 06510.

Adrian, Chandler & Hodgkin (1970) used a longitudinal voltage difference (ΔV) recorded between two microelectrodes, as a measure of membrane current (i_m) close to one end of a frog sartorius fiber. Their method is good for studying outward currents under voltage clamp but less suitable for inward regenerative current since (1) all-or-nothing responses arise in the long end of the fiber, and (2) 5% error between measured and actual i_m is exceeded for $\ell/|\lambda| = 0.65$, thus placing narrow limits on inward current magnitude or electrode spacing. These problems were dealt with in adapting the method to Purkinje fibers for the study of small inward currents partly carried by Ca ions. (1) short preparations are used so the current electrode may be placed midway between the healed-over ends. (2) the electrode spacing is modified. At best, $\alpha = 1.5$ as indicated, and measured i_m lies within 6% of actual i_m for $\ell/|\lambda| = 1.3$. This quadruples the permissible range of i_m for a given electrode spacing. The modified method also provides two measures of membrane current, ΔV and I_{total}. Theoretical calculations incorporating time-dependent inward current indicate that ΔV will always reflect i_m more accurately than I_{total}, but correspondence between these is a useful check. In preparations 2 mm long, even I_{total} may be a reasonable measure of i_m for peak inward currents ($\leq 40 \mu A/cm^2$) large enough to account for "slow responses".

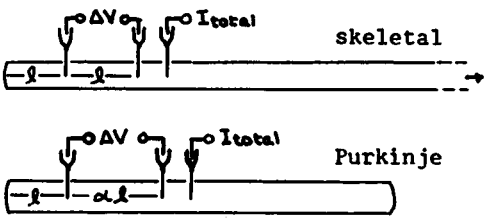

Biophysical Journal vol. 15, 1975 258a

F-AM-A13 ASSESSMENT OF THE TENSION-VOLTAGE RELATIONSHIP IN FROG ATRIAL MUSCLE. M. Tarr and J. W. Trank, Department of Physiology, University of Kansas Medical Center, Kansas City, Kansas 66103.

Recently the voltage-clamp technique has been applied to a variety of cardiac tissue to investigate the relationships between contractile activity and membrane voltage and/or membrane current. Of particular interest has been the role of the slow inward calcium current (I_s) in the phasic tension response (T_p) in frog atrial muscle. The purpose of this study was to evaluate the tension-voltage relationship of frog atrial muscle in relation to 1) I_s and 2) the limitations of the double sucrose-gap voltage clamp technique in the determination of tension-voltage and tension-current relationships. When step-clamp depolarizations were applied to frog atrial muscle under "voltage clamp" conditions, T_p appeared to be related to the magnitude of I_s in that both the T_p-clamp potential and the I_s-clamp potential relation had their maximum at approximately the same potential. However, a similar T_p-clamp potential relationship was obtained when the voltage clamp was applied during the plateau of the action potential. Microelectrode potential measurements from cells in the test node demonstrated the lack of temporal and spatial voltage control under both step-clamp and action potential-clamp conditions, and also demonstrated the presence of action potential activity under step-clamp conditions. These data indicate that contractile activity elicited by action potential activity in the "voltage clamped" region of the tissue makes a significant contribution to the phasic tension response obtained under so-called voltage clamp conditions. In light of these data, a cause and effect relationship between the slow inward calcium current and the phasic tension component in frog myocardium is not obvious. Supported by NIH Grant HL12426 and a Kansas Heart Association Grant-in-Aid.

F-AM-B1 TWO LEVELS OF RESTING POTENTIAL IN CANINE CARDIAC PURKINJE FIBERS EXPOSED TO SODIUM-FREE SOLUTIONS. J.R. Wiggins* and P.F. Cranefield.
The Rockefeller University, New York, N.Y. 10021

Canine cardiac Purkinje fibers exposed to Tris-buffered Na-free solutions containing 2.7mM K, 16mM Ca, 20 mM tetraethylammonium Cl and 108mM tetramethylammonium Cl may be rhythmically active with a maximum diastolic potential (MDP) of about -60mV or quiescent with a resting potential of either -50mV (RP_{-50}) or -90mV (RP_{-90}). In about half of the fibers studied each of these states may be evoked at will as follows. A fiber that is quiescent at RP_{-90} becomes active during a long(20sec) depolarizing pulse. At the end of the pulse the fiber may return to RP_{-90} or it may remain rhythmically active with an MDP of -60mV. Fibers that remain rhythmically active speed up during a further depolarizing pulse; at the end of such a pulse they may return to their original rate but often become quiescent at RP_{-50}. Fibers that become quiescent at RP_{-50} can be returned to RP_{-90} by application of a hyperpolarizing current; the transition from RP_{-50} to RP_{-90} may also occur spontaneously. Whether spontaneous or induced, the transition from RP_{-50} to RP_{-90} is an all-or-none phenomenon that may result from a voltage-dependent increase in P_K. The resting potential of RP_{-90} fibers varies linearly with $\log[K]_o$; the resting potential of RP_{-50} fibers is relatively insensitive to changes in $[K]_o$. When $[Ca]_o$ is less than 16mM the fibers tend to be in the RP_{-50} range, tend to be rhythmically active and cannot be easily "switched" to RP_{-90}. When $[Ca]_o$ is 16mM the fibers are more likely to be at RP_{-90} and can less often be switched to sustained rhythmic activity or to quiescence at RP_{-50}, although they usually show sustained rhythmic activity during a depolarizing pulse. Quiescent RP_{-50} fibers usually showed sustained rhythmic activity in response to the break of a brief anodal stimulus. (Supported by HL14899)

F-AM-B2 EFFECT OF LOW CA AND POLARIZATION UPON IMPEDANCE OF SPACE-CLAMPED SQUID AXONS STIMULATED BY WHITE NOISE, AS DERIVED FROM INPUT-OUTPUT CROSS CORRELATIONS. L. Feldman* and R. Guttman, Marine Biological Laboratory, Woods Hole, Mass. 04523 and Dept. of Biology, Brooklyn College of the City Univ. of N.Y., Brooklyn, N.Y. 11210.

Current from a white noise generator was applied as a stimulus to a space-clamped squid axon in double sucrose gap. The input-output relationship (impulse response) was analysed by cross correlating subthreshold stimuli and responses. From the impulse response thus obtained, it was possible to obtain the impedance loci by application of the appropriate Fourier transforms. Spectrum analysis indicated that the membrane is a tuned circuit. The sharpness of tuning increased when the membrane was depolarized and decreased when it was hyperpolarized, corroborating previous findings where sinusoidal currents were used as stimuli (Guttman and Hachmeister, 1971). Impedance loci indicated that depolarization increased the inductive reactance, a situation which is associated with a ringier axon, and that hyperpolarization had the opposite effect. Spectrum analyses showed that low Ca increased the sharpness of tuning. Impedance loci indicated that low Ca increased the inductive reactance. High Ca had opposite effects. These noise measurements corroborate and extend the classical impedance studies of Cole.

Aided by NSF Grants GB-28527 and GB-38355 awarded to RG.

F-AM-B3 IONIC CONDUCTANCE IN CRAYFISH AXONS AFTER CHEMICAL MODIFICATION OF HISTIDYL, SULFHYDRYL, AND AMINO GROUPS. Peter Shrager, Dept. of Physiology, Univ. of Rochester Medical Center, Rochester, New York 14642.

Experiments have been conducted in an attempt to find and characterize covalent modification procedures specific for different components of conductance in nerve. Earlier work showed that potassium currents are markedly slowed as the external pH is lowered, and the resulting titration curve suggested protonation of a histidyl imidazole group. Carbethoxylation of histidine by diethylpyrocarbonate (DEPC) also slowed and inhibited I_K, but had no effect on I_{Na}. Studied in perfused axons, neither low pH nor DEPC was effective when applied internally. Modification of sulfhydryl groups by N-ethylmaleimide (NEM) resulted in an inhibition of sodium currents without changes in kinetics. Potassium currents were unaffected. 5,5'-dithiobis(2-nitrobenzoic acid) (DTNB), a sulfhydryl reagent that is larger than NEM and bears a net charge (-2), has no effect when applied externally. 2-methoxy-5-nitrotropone, which reacts specifically with amino groups, has effects similar to those of NEM, but inhibition of I_{Na} is not complete. 1-fluoro-2,4-dinitrobenzene (FDNB) blocks all of the above groups and supresses ionic currents in squid axons (Cooke et al., PNAS 60:470, 1968). FDNB reduces I_{Na} in crayfish axons and also slows and inhibits I_K. This is consistent with block of sulfhydryl or amino groups (I_{Na}) and histidyl groups (I_K). Supported by N.I.H. grants 5-R01-NS10500-02 and 5-P01-NS10981-02.

F-AM-B4 OCTOPUS TOXIN BLOCKS SODIUM CONDUCTANCE IN SQUID AXON. Peter W. Gage*, John W. Moore and Monte Westerfield*, Sch. of Physiol. & Pharmacol., Univ. of New South Wales, Kensington, Australia; Dept. of Physiol. & Pharmacol., Duke Univ., Durham, N. C.

The effects of Maculotoxin (MTX), extracted from the salivary glands of the Australian Blue-ringed Octopus, have been examined by voltage-clamp techniques on squid axon. At concentrations in the 10^{-5} g/ml range, it blocks the voltage-sensitive sodium conductance channels without having any effect on the potassium channels. Whereas TTX affects only the amplitude of the sodium conductance, as MTX blocks the transient conductance, it slows the turning-on process, delays the time-to-peak and shifts the voltage at which the peak inward current occurs. MTX does not appear to change the "tail" kinetics nor affect the sodium conductance inactivation and restoration processes. The effectiveness of MTX is:

1. increased by repetitive depolarization,
2. not altered by the Ca^{++} concentration but
3. reduced as the pH is raised from 7 to 9.

F-AM-B5 INTERNAL K^+ ALTERS SODIUM CHANNEL SELECTIVITY. M. Cahalan* and T. Begenisich*. (intr. by M.F. Schneider). Department of Physiology, University of Rochester and Department of Physiology and Biophysics, University of Washington.

Using perfused, voltage clamped squid axons we have measured changes in the selectivity ratio, P_K/P_{Na}, of sodium channels as the internal potassium activity (a_K) was varied. While keeping ionic strength constant by adding impermeant tetramethylammonium ions (TMA), changing a_K from 355 to 42.5 mM produced a change in P_K/P_{Na} from 0.069 to 0.38. Changing the ionic strength with TMA at constant a_K produced little change in the reversal potential and hence in P_K/P_{Na}. Other experiments indicate that P_{Cl}/P_{Na} is less than 1/500. Changing external $[Na^+]$ shifted the reversal potential nearly in accord with Nernst potential predictions, indicating that membrane potential itself has little effect on P_K/P_{Na}. A plot of P_K/P_{Na} as a function of $1/a_K$ is linear, suggesting that K^+ ions interact with a saturable site controlling permeability, having an equilibrium constant of 750 mM.

F-AM-B6 SELECTIVE MODIFICATION OF SODIUM CHANNEL GATING BY TRINITROPHENOL. G. S. Oxford and J. P. Pooler, Dept. of Physiology and Pharmacology, Duke University Medical Center, Durham, N. C. 27710, and Dept. of Physiology, Emory University, Atlanta, Ga. 30322.

The sodium channel gating properties of lobster axons are altered by 2,4,6-Trinitrophenol (TNP) as measured using the double sucrose gap voltage clamp technique. 1 mM TNP rapidly and reversibly prolongs the time course of sodium currents during maintained depolarizations over the full voltage range of observable currents while also producing increases in peak I_{Na} in most experiments. Potassium and leakage currents are not measurably altered by TNP. The Hodgkin-Huxley inactivation time constant τ_h extracted from the decay of I_{Na} during a maintained depolarization is increased at all voltages where it is measurable. τ_m of the Hodgkin-Huxley model is not altered during activation of g_{Na}, while the removal of activation is retarded, as sodium tail currents are significantly prolonged upon repolarization. The steady-state sodium inactivation curve is shifted along the voltage axis in the hyperpolarizing direction by ≈ 14 mv, with a similar shift being observed in the inactivation time constant curve as determined by conditioning voltage steps. This shift speeds the kinetics of inactivation over part of the same voltage range in which sodium currents are simultaneously prolonged, an observation incompatible with the Hodgkin-Huxley model. These data are interpreted as evidence for two inactivation processes - one proceeding directly from the resting state and the other coupled to the decay of active sodium conductance. Supported by USPHS Grant NS09040.

F-AM-B7 BLOCK OF IONIC CHANNELS IN AXONS BY STRYCHNINE. B. I. Shapiro, Biological Laboratories, Harvard University, Cambridge, Ma. 02138

Externally applied strychnine blocks both sodium and potassium channels in membranes of frog nodes. The blockage of potassium currents is voltage and time dependent. The more positive the membrane potential the greater the block and the more rapidly the equilibrium level of blockage is attained. Pretreatment of the axon with scorpion venom reduces and greatly slows sodium inactivation, allowing the action of strychnine on sodium channels to be studied. Subsequent application of strychnine produces a voltage and time dependent block similar to that of potassium channels. The more positive the membrane potential the greater and faster the sodium channel block. A quaternary strychnine derivative, N-methyl strychnine, blocks both channels in a manner indistinguishable from strychnine, but is effective only when applied to the inside of the node. Externally applied it produces no effect on sodium currents and a moderate voltage and time independent block of potassium currents. This plus other evidence strongly suggests that externally applied strychnine acts in its charged form from the inside. It is consistent with a model in which the strychnine cation moves down the electric field to block at a site in the membrane. The strychnine probably reaches the inside by crossing the membrane in the uncharged form.

The blockage of potassium channels by strychnine is reduced by increasing the external potassium but unaffected by external sodium, lithium, or tetramethylammonium ions. The blockage of sodium channels is reduced by increasing external sodium but is unaffected by external potassium. Lithium can substitute for sodium about 1:1. This suggests that the blockage of the two classes of ionic channel by strychnine are independent though similar events.

F-AM-B8 AN INVESTIGATION OF THE EFFECTS OF TETRAETHYLAMMONIUM ION ON A TRANSIENT POTASSIUM CURRENT IN MOLLUSCAN NEURONS. D. Walter* and J.A. Connor, Department of Physiology and Biophysics, University of Illinois, Urbana, Illinois 61801.

A study has been made of the effects of tetraethylammonium ion, TEA^+, on the transient potassium current, I_A, seen in molluscan central neurons (Connor and Stevens, J. Physiol. (Lond.) 213, 1971 21-30). This current is not noticeably altered by external TEA^+ (100 mM). TEA^+ injected into the cell, however, decreases the magnitude of I_A and also significantly changes the kinetics. The time course of both rising and falling phases is slowed and the falling phase develops a strong voltage dependence, not present in the control. The rising phase shifts from one fit by a fourth power exponential to one in which a slower first order exponential is dominant. High external potassium (400 mM, Na replacement) which reverses the direction of I_A does not alter the effects of the internal TEA^+. Analysis of several possible kinetic schemes has been carried out and the one which best fits the available data is a model in which activation and inactivation processes are coupled with at least one non-conducting TEA^+-bound state adjacent to the conducting state. (Supported by NSF GB39946 and HEW PHS GM00720.)

F-AM-B9 MODIFICATIONS OF SODIUM CONDUCTANCE KINETICS OF SQUID AXON MEMBRANES BY PANCURONIUM. J. Z. Yeh and Toshio Narahashi, Department of Physiology and Pharmacology, Duke University Medical Center, Durham, N. C. 27710.

When perfused internally through the squid giant axons, 1 mM pancuronium (PC) selectively changed the sodium conductance kinetics without affecting the potassium kinetics. The initial falling phase of sodium conductance was greatly accelerated but the rising phase remained unchanged. This resulted in a 40% decrease in the peak sodium conductance. The acceleration of the falling phase of sodium conductance might, at a glance be due to an acceleration of sodium inactivation (h) of the Hodgkin-Huxley formulation. However, neither the time constant of inactivation, estimated by the double pulse technique for membrane potentials more negative than -30 mV, nor the steady-state sodium inactivation was significantly changed by PC. The PC-induced acceleration of the falling phase of sodium conductance could still be observed after treatment with pronase, which completely removed the normal sodium inactivation. These results suggest that the PC-induced acceleration requires the opening of m gates. Upon repolarization, PC induced a peculiar tail current which was characterized by an initial rising phase followed by a slow falling phase. All of these results cannot be explained by the Hodgkin-Huxley formulation. Alternatively, a slight modification of a kinetic model recently developed by J. W. Moore and E. B. Cox (personal communication) could fit the observations very well. The modified model requires the inactivation process coupled with the activation process. (Supported by NIH grant NS 10823).

F-AM-B10 SPECIFIC ACTIONS OF DEOXYCHOLATE ON THE SODIUM CHANNEL OF SQUID AXON MEMBRANES. Chau H. Wu*, Paul J. Sides*, and Toshio Narahashi, Department of Physiology and Pharmacology and Department of Pathology, Duke University Medical Center, Durham, N. C. 27710.

Deoxycholate (DOC) has long been known to cause neurologic effects. In view of its wide popularity in extraction of membrane proteins as well as its potential usefulness in studying protein-lipid interactions in excitable membranes, we have investigated its actions on squid axon membranes. When applied externally, 2×10^{-6} M DOC suppressed the amplitude and prolonged the duration of action potential without appreciable effects on the resting potential. It induced spontaneous repetitive discharges, an effect observed only at low temperatures (5-12°C). Under voltage clamp conditions DOC applied either externally or internally reduced sodium conductance reversibly without affecting potassium conductance. An apparent dissociation constant for the drug-receptor complex was estimated to be 1.75×10^{-6} M with a one-to-one binding stoichiometry. The sodium inactivation was slowed, but the steady-state sodium inactivation was unaffected by DOC. This can be interpreted as being due to the equal suppression of α_h and β_h in the Hodgkin-Huxley formulation. In terms of a recently developed kinetic model for the sodium conductance system (J. W. Moore and E. Cox, personal communications), these effects can be ascribed to DOC binding to the precursor of the conducting sodium channel to form an inactive DOC-precursor complex. (Supported by NIH grant NS 10823).

F-AM-B11 DEPENDENCE OF SQUID AXON LEAKAGE CONDUCTANCE ON TIME AND CHOLINERGIC DRUGS. Carlos Sevcik* (Intr. by J. Villegas), Centro de Biofísica y Bioquímica, Instituto Venezolano de Investigaciones Científicas (IVIC), Caracas, Venezuela.

Leakage conductance of the giant axon of the tropical squid Dorytheutis plei is not a constant. The membrane potential of the axon was electronically controlled and held at -80 mv. Leakage conductance was measured at 22° C by means of hyperpolarizing pulses. Leakage conductance decreases initially at a rate of 1.95 ± 0.06 %/minute (mean ± S.E.M., 4 nerves) during the first 20 min. This rate of change may be modified by bath application of Pronase, Phospholipase C and several cholinomimetics and litics. However, the drugs tested in the present study do not affect significantly the sodium and potassium conductances. Rates of change, higher than the control, were observed in 1 mg/ml of Pronase (5.41 ± 0.28, 10 nerves); 1 mg/ml Phospholipase C (5.02 ± 0.27, 4 nerves); Acetylcholine 10^{-6} M (2.65 ± 0.17, 3 nerves); Carbamylcholine 10^{-6}M(3.19 ± 0.07, 5 nerves) and 10^{-5} M (3.32 ± 0.08, 6 nerves); d-Tubocurarine 10^{-5} M (2.82 ± 0.13, 5 nerves) and Atropine 10^{-5} M (4.61 ± 0.18, 6 nerves). Lower rates were observed in Acetylcholine 10^{-5} M (-0.58 ± 0.18, 6 nerves); and Carbamylcholine 10^{-4} M (0.90 ± 0.01, 7 nerves). These experimental results suggest the presence of cholinergic receptors of the muscarinic type on the external surface of the axolemma. The effects of Atropine and d-Tubocurarine also suggest that Acetylcholine is normally present in the Frankenhauser and Hodgkin space.

F-AM-B12 ALTERATION OF AXON IONIC CHANNELS BY CEREBRATULUS PHOSPHOLIPASE A. W.R. Kem*, Dept. of Pharmacology and Therapeutics, Univ. of Fla., Coll. of Med., Gainesville, Fla. 32610 (Intr. by F. Bilallonga).

Phospholipase A, a major component of the toxic mucus secreted by the marine worm Cerebratulus lacteus, was purified by G-50 Sephadex and CM-cellulose chromatography and found to be homogeneous by gel electrophoresis, analytical gel chromatography, and amino acid analysis. The enzyme is highly basic (pI>8.9) and consists of a single polypeptide chain (MW 11,000). Acyl hydrolase activity is enhanced by Ca^{++}, but inhibited by low concentrations of deoxycholate or Triton-X-100 which enhance the bee venom enzyme. External application of pure Cerebratulus phospholipase A (10 µg/ml) rapidly and irreversibly blocks the action potential and depolarizes the resting membrane of squid and crayfish giant axons. Voltage clamp analysis of the effects of externally-applied Cerebratulus phospholipase A upon intact Loligo axons demonstrated a characteristic time sequence of alterations in the ionic conductances. Sodium conductance is almost entirely blocked before other conductances are significantly affected. Potassium conductance progressively decreases, and finally, the resting conductance drastically increases by as much as 100-fold. These alterations closely resemble the effects produced by internal (but not external) application of a phospholipase A from mouse intestine. The ineffectiveness of certain phospholipase preparations when externally applied to axons may be due to differences in pH, ionic, temperature, and substrate requirements, or differences in enzyme purity. The ability of low concentrations of externally-applied Cerebratulus enzyme to preferentially alter the sodium channel in intact axons suggests that it may be useful for investigating the structural interactions between phospholipids and the molecular constituents of this channel.
Supported by NIH GRS grant RR5362-11 and by a PMA Research Starter grant.

F-AM-C1 MINIATURE ENDPLATE POTENTIALS AT THE FROG NEUROMUSCULAR JUNCTION MAY BE COMPOSED OF SUMMED QUANTA. Mahlon E. Kriebel*, intr. by T. J. Csermely, Department of Physiology, Upstate Medical Center, State University of New York, Syracuse, New York 13210.

Miniature endplate potential (MEPP) amplitude histograms always show two distinct modes (small mode 2-4%) and many have a multimodal profile showing peaks that are multiples of the smallest mode. Only about 10% of the histograms show a normal shaped major mode profile. Nerve stimulation at 10 Hz progressively decreases the MEPP amplitudes until all MEPPs are of the small mode class (Kriebel and Gross, 1974, J. Gen. Physiol. 64:85). In the stressed preparation, unitary evoked potentials are of small mode size. The occurrence of small mode MEPPs (as well as all MEPPs) does not fit a Poisson distribution. Small mode MEPPs recorded from very small (6-12μ) sartorius muscle cells have a mean of 0.3 to 0.6 mv and show a normal distribution (MEPP mean 2.5-6mv). With the addition of 10-12.5 mM Mg^{++} (half Ca^{++}) the small mode mean did not appreciably change, whereas the profile of the overall amplitude histogram greatly changed. In some cases, 30% of the MEPPs were small mode. The average MEPP decreased by 50%. In Mg^{++} the unitary evoked responses, during 60% failures showed the same distribution as the spontaneous MEPPs demonstrating that small mode MEPPs are also evoked in the unstressed preparation. In addition, too many spontaneous MEPPs showed several breaks on their rising phase to be accounted for by chance coincidences. These observations suggest that the smallest mode MEPPs represent single quanta and that the larger MEPPs result from the summed release of several quanta. Supported by NIH.

F-AM-C2 BINOMIAL RELEASE OF TRANSMITTER AT MAGNESIUM-TREATED FROG NEUROMUSCULAR JUNCTIONS. M. D. Miyamoto*, D. D. Branisteanu* and R. L. Volle, Department of Pharmacology, University of Connecticut Health Center, Farmington, Conn. 06032.

Transmitter release from selected Mg^{++}-treated neuromuscular junctions in the frog can be described by binomial statistics. The probability of release (p) was estimated by

$$p = 1 - \frac{(\text{var EPP})}{\overline{EPP}\cdot\gamma} + \frac{\sigma^2}{\gamma^2}$$

where γ is the mean amplitude and σ^2, the variance of the mepp's, respectively (Bennett and Florin, J. Physiol. 238:93, 1974; Miyamoto, 1975). Quantal content (m_1) was estimated by $\overline{EPP}\cdot\gamma^{-1}$ and available stores (n) by $n = m_1 \cdot p^{-1}$. Good agreement between observed and predicted frequency-amplitude histograms of EPP's was obtained using binomial statistics when relatively low concentrations of Mg^{++} were used to depress transmission. Conversely, good agreement was found with Poisson predictions when higher concentrations of Mg^{++} were used. Similar values for p were obtained at the same junction when binomial analysis was compared with the method used by Christensen and Martin (J. Physiol. 210:933, 1970). Mg^{++} depressed the amplitude of EPP's, reduced m and p, but had no effect on n. Raising Ca^{++} increased the amplitude of the EPP's, m and p without changing n. Similarly, K^+ increased m and p but not n. During frequency-facilitation (1 to 6 Hz), EPP's, m and n were increased and p was unaffected. It is concluded that binomial statistics can be used to estimate the quantal parameters of transmitter release and that these parameters can be identified as discrete entities. (Supported by grant NS-07540-7).

F-AM-C3 DOSE-RESPONSE RELATIONSHIP AT THE FROG NEUROMUSCULAR JUNCTION. V.E. Dionne, J.H. Steinbach* and C.F. Stevens, Department of Physiology and Biophysics, University of Washington, Seattle, Washington 98195.

Information on molecular mechanisms governing postsynaptic permeability changes may be obtained from the relationship between agonist concentration and post-junctional conductance. We have measured the conductance change induced by agonists at the frog neuromuscular endplate as a function of acetylcholine and carbamylcholine concentrations. Endplate regions of Rana pipiens cutaneous pectoris muscle cells were visualized using Nomarski optics and voltage-clamped with two microelectrodes. Acetylcholine and carbamylcholine were applied iontophoretically and their concentration close to the iontophoresis source determined with an ion-selective microelectrode. Brief iontophoretic current pulses (0.1-0.2 sec, 0.1 Hz) were delivered 30 to 50 μm from the endplate to minimize receptor desensitization and maintain low agonist concentration within the synaptic cleft. The maximum agonist concentration near the source (typically measured 10 μm away) normally ranged from 10 μM to 1 mM, and it is estimated that the highest cleft concentrations were less than 1/10 this value. The responses induced by either agonist can be fit by an equation of the form $g = AC+BC^2$ where g is the agonist induced conductance change, C is the cleft agonist concentration and A and B are constants. These results are consistent with a molecular scheme in which either one or two agonist molecules may induce a receptor-channel to open.

F-AM-C4 A NON-LINEAR DOSE-RESPONSE RELATION AT THE FROG NEUROMUSCULAR JUNCTION. Richard S. Norman, Biological Sciences Group, University of Connecticut, Storrs, Connecticut 06268.

Depolarization of frog sartorius muscle fibers, as measured with an intracellular microelectrode, is a non-linear function of quantity of applied acetylcholine (ACh), there being a pronounced S-shape or toe in the dose-response relation. To avoid desensitization, ACh must be applied rapidly, hence iontophoretically, and two techniques are used to avoid non-linearities in the ejection properties of the iontophoresis electrode. First, by using the same electrode at different diffusion distances, very different currents are required, so different regions of the electrode characteristics are involved. Second, by using pulse-width modulation, the total iontophoresis charge is varied over a limited range at constant current. Dose-response curves are well represented as power functions with exponent always significantly greater than unity, and in several cases greater than two. The non-linearity is seen in ACh-induced noise amplitude, but not in the amplitude of the elementary event. It is not accounted for by electrical properties of the post-synaptic membrane, extra-junctional receptors, the spatial distribution of junctional receptors, or the activity of ACh-ase. Since it is found in junctional receptors under physiological conditions and stimulated with the natural transmitter at physiological levels (.1 to 10 mV depolarization) the non-linearity must play a role in normal synaptic function. As a consequence, traditional methods of counting quanta, or calculating the amount of ACh in one quantum, must be significant overestimates.

F-AM-C5 THE ENDOPLASMIC RETICULUM OF NEURONS AS A CALCIUM SEQUESTERING AND RELEASING SYSTEM: MORPHOLOGICAL EVIDENCE. Maryanna Henkart, NICHD, NIH, Bethesda, Maryland 20014.

The endoplasmic reticulum of the squid giant axon swells under conditions that have been shown to increase the cytoplasmic Ca concentration, e.g. soaking in artificial sea water (ASW) containing 60 mM Ca[1] or in which Na has been replaced by Li[2]. These treatments also increase the electron opacity of fixed, unstained ER membranes. If swelling is interpreted as osmotic influx of water following Ca accumulation, these results suggest that the ER may take up Ca. Further evidence suggests that the ER may release Ca in response to surface membrane depolarization: 1) Storage of axons in ASW increases the amount of Ca entering the cytoplasm with each action potential[1]. Similarly stored axons have greatly swollen ER. 2) In axons soaked in 60 mM Ca which would have swollen ER, the ER volume is much reduced after a 10 sec depolarization in ASW containing 90 mM K or after electrical stimulation for 1 min at 16 Hz. Co which blocks the Ca influx associated with action potentials[1] appears to enter the ER. Preliminary observations indicate that similar changes occur in Aplysia neurons. Freeze-fracture studies have shown that the size and distribution of intramembranous particles at junctions between the surface membrane and sub-surface cisterns of the ER are similar in muscle and neurons[3]. These observations are consistent with the hypothesis that in neurons as in muscle the electrical activity of the surface membrane may be coupled to intracellular events by Ca release from the endoplasmic reticulum.

1. Baker, et al. J. Physiol. 218, 709 (1971).
2. Baker, et al. J. Physiol. 200, 431 (1969).
3. Landis, et al. J. Cell Biol. 59, 184A (1973).

F-AM-C6 CHARACTERIZATION OF THE Ach CHANNEL FROM ELECTRICAL NOISE IN TISSUE CULTURED CHICK SKELETAL MUSCLE. F. Sachs* and H. Lecar, Laboratory of Biophysics, IR, NINDS, National Institutes of Health, Bethesda, Md. 20014.

We have previously reported (Nature 246: 214, 1973) on the kinetics and conductance of Ach channels inferred from analysis of Ach-induced current fluctuations in tissue cultured chick pectoral muscle. These data have now been extended to cover a wider range of temperature and voltage. The muscle cells were modified by colchicine and vinblastine treatment to produce spherical cells 30 to 100 μ in diameter, which were better preparations for voltage clamp experiments than the original elongated cable-like cells. The cells also have weakened contractile ability and thus less hindrance to electrode penetration. The spectrum of the current fluctuations is Lorentzian, consistent with a simple picture of random channel openings and closings. Analysis of the noise in 46 preparations leads to a value of 60 pmho for the channel conductance. The channels stay open about 5 msec at 25°, with a Q_{10} for the channel-closing rate of 7.1. The voltage dependence of the closing rate was approximately 70 mv per e-fold change at 25° with slower rate for hyperpolarization. Comparison of our results with those of Anderson and Stevens (J. Physiol. 230: 214, 1973) on the frog neuromuscular junction indicate that the dipole moment change associated with channel closing is about the same for both species, the channel conductances are of the same order of magnitude, but that the temperature coefficients and resultant free-energy barrier for the open-close transition differ between the two preparations.

F-AM-C7 RELAXATION SPECTROSCOPY OF THE ACETYLCHOLINE RECEPTOR: RESPONSES TO VOLTAGE JUMPS IN ISOLATED ELECTROPHORUS ELECTROPLAQUES. R. E. Sheridan and H. A. Lester, Division of Biology, California Institute of Technology, Pasadena, California 91125.

When nicotinic agonists are added to the solution bathing the innervated face of an electroplaque, the agonist-induced conductance depends upon the transmembrane potential (V). We have forced V to jump from one level to another in presence of a constant agonist concentration. The conductance relaxed to a steady-state appropriate to the final V. The approach to this new level is described by an exponential whose time constant does not depend on the previous V. These two findings suggest a reversible reaction in which the relaxation time constant equals the inverse sum of the first-order rate constants governing transitions between open and closed receptors. The time constants fell in the range, 0.3 to 5 msec, and varied with temperature, with V, with the nature of the agonist, and with its concentration. The Q_{10} of the time constant was 3.3, as contrasted with 1 for the steady-state conductance. Time constants increased as V became more negative. With increased agonist concentration, time constants became faster. All other conditions being equal, the time constants decreased in the order acetylcholine>carbachol>decamethonium.

The experiments were made possible 1) by a novel voltage-clamp arrangement in which low-resistance glass electrodes were used to detect fast voltage changes and high-resistance electrodes to detect slow changes; and 2) by NIH Grant NS-11756.

F-AM-C8 INCORPORATION OF EXOGENOUS ACETYLCHOLINESTERASE INTO SYNAPTIC VESICLES IS ASSOCIATED WITH INHIBITION OF SYNAPTIC TRANSMISSION IN FROG SARTORIUS NMJ. A. L. Politoff*, A. L. Blitz*, S. Rose* (intr. by W. C. Ullrick), Dept. of Physiology, Boston Univ. School of Medicine, Boston, Mass. 02118, and Dept. of Neurobiology, Albert Einstein School of Medicine, New York, N.Y. 10461.

Frog sartorius neuromuscular junctions (NMJ) incubated for 4 hours in Ringer's solution containing 0.5 mg/ml of electric eel acetylcholinesterase (AChE) did not show detectable inhibition of synaptic transmission if the nerve was stimulated at 2/min. This result shows that exogenous AChE does not inactivate the transmitter in the synaptic gap. However, stimulation at 20 Hz for 25 min followed by a rest period of 45 min in Ringer's + AChE caused a large diminution or abolition of the responses (both muscle contraction and end plate potential) recorded during a second period of stimulation. Miniature end plate potentials were still present. AChE inactivated with paraoxon (an irreversible organophosphorus inhibitor) did not cause inhibition of transmission. Electron micrographs of NMJ's inactivated with AChE as above, and stained for AChE activity, show esterase activity in 15-30% of the synaptic vesicles. The results suggest that releasable acetylcholine is contained within synaptic vesicles.

F-AM-C9 PERIPHERAL INHIBITION IN THE MOLLUSC SEA HARE, APLYSIA CALIFORNICA. F. Banks* (Intr. by D. Junge.) Department of Biology, University of California at Los Angeles, Los Angeles, California 90024.

The innervation of the lower extrinsic protractor muscle in the buccal mass of Aplysia californica was investigated by using $CoCl_3$ as the marker precursor. The muscle was shown histologically to be innervated by three neurons in the right buccal ganglion. The functional interactions of these neurons were studied by penetrating the cell bodies and the muscle membrane with microelectrodes. A bridge circuit was used to stimulate and record from the nerve cell bodies. Low level stimulation of the root which connects the ganglion to the muscle causes E.J.P.'s in the muscle syncytium. Excitation at one of the histologically identified nerve cells causes hyperpolarizing potentials in the muscle. When this cell was excited during a root evoked muscle E.J.P., the E.J.P. was inhibited. It is possible that some of the inhibition is mediated pre-synaptically; however, the time course of the inhibited E.J.P. suggests it is mainly post-synaptic. This is apparently the first account of neuromuscular inhibition in mollusca.

F-AM-C10 SOME PROPERTIES OF MEMBRANE BOUND ACETYLCHOLINE RECEPTOR FROM RAT CEREBRAL CORTEX. C.H. McQuarrie* and H.R. Mahler*, Intr. by D.A. McQuarrie, Department of Chemistry, Indiana University, Bloomington, Indiana 47401.

A total membrane particulate fraction was derived from rat cerebral cortex by centrifugation of the supernatent obtained after removal of myelin. The acetylcholine receptor was assayed by its ability to bind ^{125}I-α-bungarotoxin, a neurotoxin component of the venom of the Elapid snake, Bungarus multicinctus, which is known to bind specifically and essentially irreversibly to the nicotinic cholinergic receptor. Binding of the toxin showed saturation with increasing toxin concentration and constant particulate protein concentration. A Scatchard plot of the data indicated a high affinity site and a lower affinity site. The number of high affinity binding sites, as determined from the Scatchard plot, was 13×10^{-15} moles/mg. protein. After incubation with the degradative enzymes, trypsin, phospholipase A, phospholipase C, and neuraminidase, for 1 hour, the binding of toxin was reduced 35%, 60%, 85%, and 50%, respectively. The lectins, concanavalin A and fucose binding protein, reduced the binding 0% and 45%. The inhibition curves for the cholinergic drugs, tubocurarine, atropine, decamethonium, carbamylcholine, and neostigmine bromide, were determined.

F-AM-C11 ACTIVATION AND DESENSITIZATION OF THE CHOLINERGIC RESPONSE OF NORMAL AND DENERVATED FROG SARTORIUS MUSCLE. H.R. Guy (Intro. by C. Edwards), Department of Biological Sciences, State University of New York at Albany, Albany, New York, 12222.

A method has been developed for determining the dose-response relationship for both activation and desensitization of the change in membrane conductance, G(C,t), of the frog sartorius muscle in the presence of ACh. Following a step increase in the concentration, C, of ACh the membrane voltage response, measured with the moving electrode technique, rapidly reaches a peak value after which it decays slowly to a steady state level. G(C,t), which was calculated from the membrane voltage response, is thus a function of C and of the duration of exposure, t, to ACh. In our analysis it was assumed that G(C,t) can be expressed as G(C,t)=A(C,t)D(C,t) where A(C,t) is a measure of the response in the absence of desensitization and D(C,t) reflects the desensitization. The kinetics of the onset of activation and desensitization are consistent with the assumption that when the peak response is reached following a step increase in C, D(C,t) has not changed significantly while A(C,t) has reached its steady state value, A(C,ss). Using these assumptions A(C,ss) and D(C,ss) were calculated from the values of the peak and steady state membrane voltage responses to successive step increases in C. The data indicate that activation is satisfied by the equation $A(C,ss)/[A(max,ss) - A(C,ss)] = K_{\frac{1}{2}}C^n$. For normal muscles $K_{\frac{1}{2}} = 90 \pm 50\ M^{-1}$ and $n = 1.2 \pm .2$ while for denervated muscles $K_{\frac{1}{2}} = 2.5 \times 10^4\ M^{-1}$ and $n = 1.0$. The function D(C,ss) has not been fit satisfactorily by a simple equation. Supported by USPHS grant NS 07681.

F-AM-C12 EFFECT OF CROSS-REINNERVATION ON FAST AND SLOW MUSCLES OF RABBIT. F.A. Sréter, A. Luff* and J. Gergely, Dept. of Muscle Res., Boston Biomedical Research; Dept. of Neurol., Mass. Gen. Hosp.; Depts. of Neurol. and Biol. Chem., Harvard Med. Sch.; and Dept. of Physiol., Univ. Bristol, U.K.

Physiological and biochemical studies on cross reinnervated fast (ext. dig. long., EDL) and slow (Soleus, SOL) twitch muscles of the rabbit showed good fast↔slow conversion 11 months after surgery. Average values of intrinsic shortening velocity (V), twitch time to peak (t), Ca^{2+} uptake (ΔCa), rate of Ca^{2+} uptake (R_{Ca}) by fragmented sarcoplasmic reticulum (FSR), and Ca-activated myosin ATPase are shown below for control (C), self (S) and cross (X) reinnervated muscles. The table also contains data concerning the effect of exposure to pH 9.2 on myosin ATPase (ALK ATPase) activity:

	C-EDL	S-EDL	X-EDL	N-SOL	S-SOL	X-SOL
V, $\mu m\ s^{-1}$	40.2	46.2	21.6	17.3	19.1	39.2
t, s	23	21	53	60	64	24
R_{Ca}, $\mu mol\ mg^{-1}\ min^{-1}$	1.26	1.64	0.30	0.33	0.22	0.63
ΔCa, $\mu mol\ mg^{-1}$	2.67	3.65	0.89	0.72	1.00	2.06
M-ATPase, $\mu mol\ mg^{-1}\ min^{-1}$	0.66	0.66	0.31	0.17	0.19	0.50
ALK ATPase, $\mu mol\ mg^{-1}\ min^{-1}$	0.65	0.66	0.29	0.05	0.05	0.49

It appears that essentially complete physiological conversion was accompanied by partial biochemical conversion as judged by the FSR and myosin characteristics. SDS-gel electrophoretic examination of the myosin light chain pattern also showed only partial fast↔slow conversion on cross-reinnervation. In contrast, chronic stimulation for 15 weeks of a fast (tib. ant.) muscle (Sréter et al, in press) produced complete biochemical transformation as judged by the above criteria.

F-AM-D1 WAVES ELICITED FROM PERIPHERAL NEURAL TISSUE (OLFACTORY) IN RESPONSE TO ODOROUS STIMULATION. Don Tucker, Department of Biological Science, Florida State University, Tallahassee, Florida 32306.

Electrical waves, having no relation to EEG type waves of the CNS, can be obtained routinely from the olfactory organ and nerve of land turtles. This result, heretofore unreliable, was achieved by assisting respiratory ventilation. Peripheral olfactory waves have been reported over the past 20 years from amphibians, reptiles, birds and mammals. Some species apparently tolerate less anoxia for a given anesthetic dosage and in these the waves were seen occasionally. A student (R. Beuerman) observed the peripheral waves routinely in Gopherus polyphemus with little enough urethane to obtain olfactory bulb responses. Because waves were almost never seen in hundreds of Terrapene carolina specimens at our standard dose rate of 2.5 g/kg, this preparation was studied with barbiturates, chloral hydrate, Halothane and combined spinal-midbrain sections. Appearance of the waves correlated with more frequent respiratory movements and they persisted at higher anesthetic doses with artificial respiration. Failure of the waves at high doses in spite of forced ventilation appeared to be due to depression of cardiac activity. With minimal or no anesthesia the waves could not be adapted out by repeated stimulation. They appeared in the nerve as a partial synchronization of the axonal spike activity. Unit recordings in the olfactory mucosa by microelectrode revealed grouping of spikes in the negative half cycles of the waves superimposed on the electro-olfactogram (EOG); a monophasic, negative odor response. An apparent wave threshold above the odor response threshold, observations of voltage sensitivity of the neuronal receptors and the absence of synapses suggest that the mechanism is self stimulation of the olfactory organ by the EOG voltage wave. Supported in part by NS 08814.

F-AM-D2 A MODEL OF COCHLEAR FUNCTION. T.W. Barrett, Department of Physiology & Biophysics, University of Tennessee Center for the Health Sciences, Memphis, Tennessee 38163.

Recent analyses in structural information theory (Barrett, Biophysical Soc. Abs. (1973) & (1974); J. Acoust. Soc. Am., 54 (1973) 1092-8) indicate the cochlea analyzes concurrently an acoustical signal's center frequency (f_o), midperiod (t_o), bandwidth (Δf) and also its duration (Δt), so that for a minimum an elementary signal is obtained: $\Delta f.\Delta t = f_o.t_o = 1/2$. The present analysis extends this investigation to cochlear models. Because the basilar membrane decreases in thickness from base to apex while increasing in width, by dimensional analysis the problem of cochlear sound reception is analogous to that of a wave breaking on a beach. Unfortunately, the latter hydrodynamic problem has been solved only for a few instances and no generalized solution exists. Another dimensional analysis suggests that cochlea dynamics are analogous to those of a shock wave in a gas. In this situation the medium is considered isentropic and amenable to treatment by field equations. A model for the cochlea is thus obtained based on flow, the Hugoniot relations and impedance resonance. The model accounts for spatial or Fourier dispersion of frequencies and effects a distinct representation of elementary signals versus sinusoids, indicating a Laplace transformation of signals such that sinusoids and sinusoidal components of elementary signals are represented on a Fourier (imaginary) longitudinal axis, and 1/2 octave bandwidth components of elementary signals on a transverse (real) axis. The present model differs from others as follows: 1) it is neither an electrical network nor a phenomenological model; 2) it accounts for two-dimensional cochlea forces rather than merely one-dimensional; 3) the forces acting on the basilar membrane are calculated analytically rather than by boundary condition methods.

F-AM-D3 THE ROLE OF AN ELECTROGENIC SODIUM PUMP IN BARORECEPTOR FUNCTION. W. R. Saum* and A. M. Brown (Intr. by A. D. Kenny), Dept. of Physiology & Biophysics, Univ. of Texas Medical Branch, Galveston, Texas 77550.

Baroreceptors show adaptation to a step-pressure increase and post-excitatory depression (PED) following removal of the stimulus (Landgren, 1952). Ouabain, which blocks membrane Na-K ATPase, elicits a reflex bradycardia probably by increasing baroreceptor discharge (Quest & Gillis, 1971). Hence we examined the possibility that an electrogenic Na^+ pump is involved in adaptation and PED. Single unit afferent recordings were obtained from slips of fibers dissected from the aortic nerve of an isolated, perfused rat aortic-arch preparation. Baroreceptors examined under these conditions showed the usual pressure-response characteristics to a square wave pressure step, i.e., threshold (60-120mm Hg), an S-shaped curve with saturation and adaptation. Hysteresis was negligible. Many receptors showed a steady-state neural discharge (15c/s to 75c/s) at pressures above threshold. A second pressure step elicited an increased discharge which adapted to a new steady-state level. Return to the initial pressure level was accompanied by PED of variable duration (for as long as 10 sec.). PED could also be produced by electrical stimulation (25c/s to 150c/s) of the aortic nerve with a separate pair of bipolar electrodes. PED was linearly related to the number of preceding impulses which could be introduced mechanically (pressure step) or electrically (antidromic stimulation). During PED the nerve trunk still conducted electrically-evoked action potentials and an increased pressure step elicited a neural discharge. PED was reversibly blocked by ouabain ($1x10^{-4}M$) and zero K^+ Krebs-Henseleit solution. These agents also increased the steady-state neural discharge. We conclude that an electrogenic Na^+ pump is responsible for PED and at least some of the adaptation observed in baroreceptors.

F-AM-D4 CHARACTERISTICS OF THE RF-SOUND TRANSDUCER. Edwin S. Eichert* and Allan H. Frey, Randomline, Inc., County Line & Mann Roads, Huntingdon Valley, Pa. 19006

Appropriately pulse modulated UHF electromagnetic energy is perceived as "sound" by humans. This phenomena, called rf-sound, can be used as a tool to investigate the auditory system. In this presentation, we will report on a psychophysical experiment designed to provide information on the characteristics of the rf-sound transducer. Humans were illuminated with pulse pair modulated 1.254 GHz electromagnetic energy. We found that the periodicity pitch phenomena is not a characteristic of rf-sound. We also found that pairs of rf pulses are perceived as equivalent to a 5 ± 1.6 KHz audio signal and that the rf-sound transducer may require at least 2 ms and possibly 3 ms for full recovery. These results will be related to other rf-sound characteristics, such as lack of cochlear microphonics, and the implications will be discussed.

F-AM-D5 BACTERIAL RHODOPSIN: A MODEL PHOTOCHEMICAL SYSTEM. Jerome J. Wolken and Christopher S. Nakagawa*, Biophysical Research Laboratory, Carnegie-Mellon University, Pittsburgh, Pennsylvania 15213.

The very halophilic bacteria grow in high salt concentrations, at high light intensity and at high temperatures. They synthesize large quantities of C_{40}-carotenoids including C_{50}-bacterioruberins, many which we have isolated from Halobacterium halobium. Of particular interest was the isolation and identification of retinal$_1$, the chromophore of visual pigments. The isolated retinal$_1$ could complex with the visual protein opsin from animal retinas to form rhodopsins (Biochem. Biophys. Res. Comm. 54, 1262, 1973). It was also found that a rhodopsin is associated with the cell "purple" membrane. These findings raise questions as to the function, if any, of retinal and rhodopsin in these bacteria. Several hypotheses which we are investigating are that it prevents photodestruction at high light intensity and temperature, that it is a repair mechanism for its DNA, and that it functions as an ion pump in the organism's energetics. To find out more about bacterial rhodopsin a variety of experiments using light and chemical reagents were carried out. The rhodopsin membranes were isolated using sucrose density gradient fractionation. The absorption spectrum of the isolated membranes has two major absorption peaks, one around 280 nm and another near 560 nm, near that of the cone pigment iodopsin. The bacterial rhodopsin does not bleach in the light and its behavior is much like squid rhodopsin. But bleaching is possible with several chemical reagents with or without light. The results indicate that retinal is attached to lysine and the bond is surrounded by a hydrophilic environment which can be altered with light. The fact that these bacteria synthesize retinal$_1$ and possess a rhodopsin-containing membrane provides a readily available model system for photochemical studies of visual pigments.

F-AM-D6 RETINAL ANALOGUES AND ARTIFICIAL VISUAL PIGMENTS. T. Ebrey, R. Govindjee, B. Honig, R. Crouch, T. Yudd, and K. Nakanishi. Departments of Physiology and Biophysics, University of Illinois, Urbana, Illinois; Physical Chemistry, Hebrew University, Jerusalem; Chemistry, Columbia University, New York, New York.

Several analogues of retinal have been synthesized and their properties as free molecules in solution investigated. Because of steric hindrance due to the presence of the extra methyl group, 11-cis, 14-M retinal cannot assume the crystal conformation of 11-cis retinal. Instead, it is in either a very highly twisted 12-s-cis or, more probably, twisted 12-s-trans conformation. As a consequence, the s-cis red shift predicted for the 11-cis isomer of retinal is absent and the absorption maximum is at 340 nm, 30 nm to the blue of 11-cis retinal. In contrast to the differences between the 11-cis isomers of retinal and 14-M retinal, the pigments they form have very similar absorption and circular dichroism spectra and photosensitivity. Other retinal analogues capable of forming pigments that will be discussed include 6-7-8 allenic retinal that cannot racemize about the 6-7 band and retinals with modified chain lengths.

F-AM-D7 STUDY OF STRUCTURE AND STRUCTURE CHANGE OF RHODOPSIN IN SITU. N. W. Downer* and S. W. Englander Department of Biochemistry, University of Pennsylvania, Philadelphia, Pennsylvania.

Hydrogen exchange methods were used to study the structure of rhodopsin in disk membranes and structure changes induced by illumination. A large fraction, about 75%, of the peptide groups of the disk membrane proteins were recognized by their hydrogen exchange rate to be freely exposed to solvent water. This contrasts with the small fraction of exposed peptides, about 30%, found for aqueous proteins and membrane systems. Significant hydrophobic interaction of rhodopsin with lipid is indicated by the proteins apolar nature and by the fact that it penetrates into the bilayer and can be removed only by the use of detergents. This together with our observation of the extensive contact of rhodopsin's peptides with water seems to require that a considerable part of the polypeptide chain be arranged at a lipid-water interface. We suggest that this interface may be the surface of a rather wide aqueous channel which penetrates into the lipid bilayer and which may play a role in the suspected transmitter release function of rhodopsin. Light-induced changes were seen to involve only slowly exchanging protein hydrogens from the structured (chromophore binding) region. Two altered forms were recognized in frog disk membranes. One is characteristic of opsin. The earlier arising deformation could be associated with either Meta II or Meta III, and therefore might be visualized to control the efflux of transmitter molecules through the channel. (Supported by N.I.H. research grant AM 11295)

F-AM-D8 ALKYL GLUCOSIDES AS EFFECTIVE DETERGENTS FOR THE SOLUBILIZATION OF BOVINE RHODOPSIN: A COMPARISON WITH SEVERAL COMMONLY USED DETERGENTS. G.W. Stubbs* and Burton J. Litman (Intr. by C. Huang), Department of Biochemistry, University of Virginia School of Medicine, Charlottesville, Va.

Of the detergents generally employed in the purification of bovine rhodopsin, none satisfies simultaneously the three requirements of being obtainable as a well defined molecular species, being transparent in the deep ultraviolet to facilitate optical studies, and being readily removable by dialysis for reconstitution experiments. Two alkyl glucosides (octyl- and decyl-β-D glucoside), whose properties conform to the above requirements, were synthesized and compared to CTAB, LDAO, Emulphogene, and digitonin as solubilizing agents for rhodopsin. The criteria studied included thermal stability of the 500 nm absorption band, regenerability by addition of 11-cis retinal to solubilized bleached rhodopsin, and the rate of change of protein conformation following bleaching. Results indicate that decyl-β-D-glucoside is second only to digitonin while octyl-β-D-glucoside is either better than or equivalent to emulphogene. LDAO and CTAB are the poorest of the detergents yielding 94% and 100% thermal bleaching respectively, when incubated at 42° for 70 min; this is to be compared to 7%, 9%, 15% and 17% bleaching for decyl-β-D-glucoside, digitonin, Emulphogene BC-720, octyl-β-C-glucoside respectively. LDAO and CTAB also gave the most rapid conformation change upon bleaching and the poorest regeneration. Our results show that the alkyl glucosides, in addition to having the desirable operational properties delineated above, are generally more mild with respect to structural perturbation of rhodopsin than many of the detergents in general use now. (Supported by UPHS Grant Ey000548 from the National Eye Institute and NSF Grant GB-41313.)

F-AM-D9 X-RAY DIFFRACTION OF DISORDERED MULTILAYERS: APPLICATION TO INTACT RETINAL ROS AFTER BLEACHING. S. Schwartz, E.A. Dratz & J.K. Blasie, Div. of Nat. Sci., U. of Cal., Santa Cruz, CA & Johnson Res. Found., U. of Penn., Phila., PA

Our previous analysis of dark adapted ROS lamellar diffraction(1974 abs.) has shown that the lattice disorder is ± 19Å out of a 295Å lattice repeat and that the substitution disorder (variation of intra-disk gap) is ±8Å out of the 88Å disc membrane center to center distance. As Chabre & Cavaggioni point out [Nat. New Biol., 244, 188 (1973)] lattice disorder increases to a higher level by 3 minutes after bleach at 22°C before returning to dark levels within 15 minutes. Applying our disorder analysis to their data we find that lattice disorder increases to ±25Å with the lattice repeat and substitution disorder staying constant. The intensity at high angles shows peaks at h/40Å [Blaurock & Wilkins, Nature, 223, 906 (1969); Corless & Costello, unpub.] indicative of the single membrane transform which is expected for the form of substitution disorder we postulated.

Our disorder analysis allows a clear separation of membrane structural changes from lattice and substitution disorder changes. In addition, we have shown that uncertainties in the 2nd order intensity and camera background for the dark adapted data do not affect the phase choice or electron density profile previously obtained. Hence, work now centers on analysis of membrane structural change upon bleaching.

F-AM-D10 SLOW BLEACH-INDUCED BIREFRINGENCE CHANGES IN ROD OUTER SEGMENTS. M.W. Kaplan*, P.A. Liebman, and C.M. Kemp*, Dept. of Anatomy, Univ. of Pennsylvania, Philadelphia, Penna. 19174.

Rod outer segments (ROS) exhibit a complex pattern of slow changes in birefringence (BR) following pigment bleach by a saturating flash. The rapid 3-4% loss of intrinsic BR concurrent with metarhodopsin II formation is followed by a further ½-1% intrinsic BR loss having a $t_{\frac{1}{2}}$(22°C) of 5-10 sec. In osmotically intact ROS attached to edge-folded retinae, the BR then rises exponentially with a $t_{\frac{1}{2}}$(22°C) of 300-400 sec to a level 3-9% higher than the pre-bleach BR. The kinetics of this BR over-recovery is similar to the kinetics of retinol formation. The BR of ROS not osmotically intact does not over-recover, but does return to the pre-bleach level at a rate close to that of metarhodopsin II disappearance. Qualitative differences are produced in the BR changes by replacing Na^+ by K^+ in the bathing medium, or by adding 110mM NH_2OH. No noticeable effects are produced by using Na^+-free(Choline-substituted), Ca^{++}-free (1mM EDTA), 5x normal Ca^{++} (10mM), Cl^--free ($SO_4^=$ substituted) or 10μM ouabain Ringer solutions. The BR changes exhibited by glutaraldehyde-fixed ROS are the same as those of ROS not osmotically intact, even though the net pre-bleach BR is reduced. These results indicate that slow photo-product related membrane structure changes and osmotically dependent morphology changes occur in ROS as a consequence of the thermal reactions of pigment bleaching.

F-AM-D11 LIGHT DISSOCIATES ENZYMATICALLY-CLEAVED RHODOPSIN INTO TWO DISSIMILAR FRAGMENTS. J.S. Pober* and L. Stryer, Department of Molecular Biophysics and Biochemistry, Yale University, New Haven, Connecticut 06520.

Thermolysin cleaves rhodopsin in retinal disc membranes into two large membrane-bound fragments. Fragment 1 (F1), which has an apparent molecular weight of 30,000 according to SDS-acrylamide gel electrophoresis, contains a binding site for concanavalin A. Fragment 2 (F2), which has an apparent molecular weight of 18,000, contains an N-retinyl group after borohydride reduction of cleaved rhodopsin. F2 also contains the accessible sulfhydryl group that reacts with the fluorescent reagent N-(iodoacetamidoethyl)-1-aminonaphthalene-5-sulfonate. F1 and F2 have similar amino acid compositions except that F1 is richer in leucine and F2 is richer in lysine. Another difference is that F1 is much more extensively labeled by ^{14}C-iodoacetate in SDS than is F2. Thermolysin also cleaves purified rhodopsin in 0.5% Triton X-100 to give F1 and F2. Thermolysin-cleaved rhodopsin in Triton X-100 has the same 500 nm absorbance as native rhodopsin. Light dissociates thermolysin-cleaved rhodopsin into F1 and F2, which can be separated by affinity chromatography on Con A-agarose. The photodissociation of F1 and F2 may be an expression of conformational changes that are part of the mechanism of visual excitation. This work was supported by a grant from the National Eye Institute (EY-01070). J.S.P. is a trainee of the Medical Scientist Training Program (GM-02044).

F-AM-D12 EFFECTS OF pH AND CO_2 ON LARGE BARNACLE PHOTORECEPTORS. H. Mack Brown and Robert W. Meech*, Department of Physiology, University of Utah College of Medicine, Salt Lake City, Utah 84132 and Zoology Department, University of Cambridge, Cambridge, England.

A short burst of HCO_3-buffered barnacle saline equilibrated with 100% CO_2 (pH 5.5) produces: 1) an immediate membrane depolarization, 2) a large decrease in resting membrane conductance, and 3) reversibly abolishes the depolarizing receptor potential of B. eburneus photoreceptors. Decreasing the external pH to the same level with other buffers (Tris, phthalate or PO_4) or increasing pH to 8.8 ($Na_2B_4O_7$) does not produce comparable effects. Thus, these changes are most likely due to an intracellular change in pH. Current-voltage (I-V) relations of the membrane obtained during application of CO_2 indicate that membrane conductance is altered significantly over the membrane potential range of -120 mV to +40 mV. The depolarizing receptor potential was not restored by applying current to hyperpolarize the membrane to the pre-CO_2 level. The depolarization and membrane conductance change produced by CO_2 were not appreciably altered by altering the amount of Cl^-, Na^+ or Ca^{++} in the external saline, but I-V relations of the membrane in different concentrations of external K^+ indicate that the membrane depolarization and decrease of membrane conductance produced by CO_2 in darkness is largely due to a decrease in K^+ permeability. Preliminary experiments on the light sensitive component of membrane conductance indicate that CO_2, or the intracellular change in pH it may produce does not exert its major effect by altering the photochemical events of visual transduction. Rather, the effects appear to be a consequence of alteration of membrane sites or carriers necessary for the normal Na-conductance increase produced by illumination. Supported by USPHS Grant EY00762.

F-AM-E1 ANTHROYL STEARATE AS A FLUORESCENT PROBE OF A CHLOROPLAST MEMBRANE ENERGIZED STATE RELATED TO PHOTOPHOSPHORYLATION. D.L. VanderMeulen and Govindjee, Departments of Physiology and Biophysics and Botany, University of Illinois, Urbana, Illinois 61801.

Chloroplasts supporting cyclic (PMS) electron flow demonstrate a reversible, light-induced enhancement of the fluorescence of the "hydrophobic probe" (12-(9-anthroyl)-stearic acid (AS) which is suppressed by phosphorylating conditions (ADP, P_i, Mg^{2+}) but completely inhibited by the uncouplers nigericin and NH_4Cl, as well as the ionophores gramicidin-D (at low concentrations) and valinomycin (at higher concentrations). A preliminary correlation (FEBS Lett. 45 (1974) 186-190) of AS fluorescence with a diffusion-potential stimulation of ATP synthesis based on the increase observed in AS emission in the dark upon addition of high concentrations of valinomycin may not be valid since valinomycin was found to modify AS fluorescence in solution. Experiments will be reported which enable a better characterization of the relationship of AS fluorescence changes to the energy transduction mechanism of photosynthesis: (i) dose responses of several ionophores, uncouplers and energy transfer inhibitors for the AS fluorescence change compared to the corresponding concentration curves for the rates of ATP synthesis; (ii) the pH dependence of the AS response in comparison with proton pumping and the fluorescence quenching of the probes 9-aminoacridine and atebrin; (iii) the effects of artifically imposed proton and salt gradients on the fluorescence of AS in solution. On the basis of this data, it appears that in chloroplast membranes AS monitors a step related to the development of the "protonmotive force", rather than a "late" step of the photophosphorylation reaction as specifically inhibited by Dio-9 or phlorizin.

F-AM-E2 TRANSFORMATIONS OF CF1-BOUND NUCLEOTIDES AND NON-PARTICIPATION OF CONVENTIONAL ADENYLATE KINASE IN THESE REACTIONS. E. N. Moudrianakis and M. A. Tiefert, Department of Biology, The Johns Hopkins University, Baltimore, Maryland 21218.

The coupling factor of photophosphorylation isolated from spinach chloroplasts (CF1) can form tight complexes with two molecules of either ADP or ATP or *pyro*phosphate, but does not appreciably bind either AMP or *ortho*phosphate. Study of the competition between ADP, ATP and *pyro*phosphate for binding to CF1 shows that the enzyme has at least three ligand-binding sites. Nucleotide that binds as ADP is converted to a mixture of CF1-bound AMP, ADP and ATP. This transphosphorylation reaction (*Proc. Nat. Acad. Sci. 68:*464 (1971)) is not due in any way to contamination of CF1 with adenylate kinase. This was established by the use of selective inhibitors and by analysis of the distribution of the reaction products found in the free soluble phase of the reaction mixture and within the 90 Å domain of the CF1 enzyme. In reaction mixtures in which CF1 was deliberately contaminated with isolated chloroplast adenylate kinase, ATP production by the two enzymatic activities could be differentiated with suitable inhibitors. In the course of these binding studies, a novel hydrolytic activity catalyzed by CF1 was discovered.

F-AM-E3 EPR STUDIES ON A HIPIP-TYPE IRON-SULFUR CENTER IN THE SUCCINATE DEHYDROGENASE SEGMENT OF THE RESPIRATORY CHAIN. T.Ohnishi*, D.B.Winter, and T.E.King, Johnson Research Foundation, University of Pennsylvania, Philadelphia, Pennsylvania 19174, Department of Chemistry, State University of New York at Albany, Albany, New York 12222.(Intr.by J.Williamson)

In addition to the two species of ferredoxin-type iron-sulfur centers [Center S-1 (Beinert and Sands, B.B.R.C.,3,41,1960) and Center S-2 (Ohnishi et al.,B.B.R.C.,53,231,1973)], a Hipip-type iron-sulfur center (Center S-3) was detected in the particulate succinate-ubiquinone reductase at the concentration equivalent to that of flavin, but was not detected in the succinate dehydrogenases (Beinert et al.,B.B.R.C.,58,564, 1974). The midpoint potential of Center S-3 was determined potentiometrically (Dutton,B.B.A.,63,1971) as + 60 ± 15 mV in the particulate antimycin A sensitive succinate-cytochrome c reductase. Upon solubilization of succinate dehydrogenase from the membrane, Center S-3 becomes extremely labile towards oxygen or other oxidizing reagents, its loss paralleling the loss of reconstitutive activity. Thus Center S-3 can be detected only in the reconstitutively active enzyme, which can transfer electrons to ubiquinone and the cytochrome chain. Even freshly prepared reconstitutively active enzyme can also have a broadened and somewhat diminished absorbance, indicating the presence of some modified enzyme. All reconstitutively inactive dehydrogenases (4 or 8 iron per flavin) have no unmodified Center S-3 absorbance. These observations indicate that Center S-3 is a constituent of succinate dehydrogenase and plays a role as an electron carrier between iron-flavoprotein and ubiquinone. (supported by USPHS grant GM-12202, GM-16767, HL-12576 and NSF grant GB-42817).

F-AM-E4 THE RIESKE IRON-SULFUR CENTER OF MITOCHONDRIA - IS IT A HYDROGEN CARRIER? Roger C. Prince* and P. Leslie Dutton* (Intr. by A.W. Kozinski), Johnson Research Foundation, University of Pennsylvania, Philadelphia, Pa. 19174.

The EPR detectable signal at g 1.90 in mitochondria was first demonstrated by Rieske et al. (J. Biol. Chem. 239, 3017) and identified as a reduced iron sulfur center. It has subsequently been shown to have oxidation-reduction midpoint potential of +280 mV at pH 7 (Wilson and Leigh, Arch. Biochem. Biophys. 150, 154); more recently the signal has been detected in a variety of organisms. It has been suggested that this iron-sulfur center might act as a chemiosmotic hydrogen carrier in the site II region of the mitochondrial electron transport chain. If this were the case, the midpoint potential of the protein would be expected to vary by -59 mV per unit increase of pH. We have been unable to detect such a shift in the range pH 6.3 to pH 8.3, indicating the oxidation and reduction of the Rieske component at physiological values of pH does not involve a proton. These results would appear to rule out the possibility that the Rieske iron-sulfur center might act as a chemiosmotic hydrogen carrier between cytochromes b and c_1 in mitochondria. In addition, we have been able to identify analagous signals in the photosynthetic bacteria Rhodopseudomonas capsulata and Rps. spheroides. The midpoint potentials of their signals are +310 mV and +285 mV respectively, and neither showed any variation with pH between pH 5.8 and 8.2. This would rule out any possibility that the Rieske centre in these organisms was a proton carrier. Supported by PHS GM 12202 and NSF GB 28125.

F-AM-E5 A RESONANT ENERGY-HYDROGEN TRANSFER THEORY OF MITOCHONDRIAL CONTROL: N. Ressler, Departments of Pathology and Biochemistry; University of Illinois Medical Center, Chicago, Illinois 60612.

Reactions between NADH, and oxidized FMN and cytochrome c were utilized as a model for studies of the theory that the coupling of resonant energy to hydrogen transfers has a fundamental biological role (J. Theoret. Biol. 23, 425, 1969). Action spectra for the photooxidation of NADH and reduction of FMN and cyt c were found to have shapes similar to the absorption spectra. Resonant energy transfers from NADH to FMN, and from FMN to cyt c were suggested by the quenching of NADH fluoresence by FMN, and of the FMN fluoresence by cyt c. If these oxidation-reduction reactions can be activated *in vitro* by excitation energy, and if this excitation energy can be transferred in the same direction as the hydrogen or electron transfers, it is possible that such a mechanism can be utilized for control of mitochondrial functions *in vivo*. The ability of this mechanism to account for interactions involved in the synthesis of ATP, respiratory control, and uncoupling are discussed. Extended excited state lifetimes would not be required. If hydrogen ions act, not literally as in an electric condenser or battery, but to induce the formation of high energy conformations, then portions of both Mitchell's chemiosmotic and Boyer's conformational theories of respiration could be involved in a single process. Such an association of energy uptake or liberation with hydrogen exchanges would be consistent with a coupling in which hydrogen transfers serve as traps in the transfer of resonant energy.

F-AM-E6 MECHANISMS OF REDUCTION OF CYT(III)C BY ONE ELECTRON DONORS. M.G. Simic, I.A. Taub*, and P.A. Hurwitz*, Food Engineering Laboratory, US Army Natick Laboratories, Natick, Massachusetts 01760

Rate constants for the reduction of cytochrome(III)c by 20 stable and unstable free radicals, generated pulse radiolytically, have been determined, and they vary with the nature of the electron donor. For aromatic radicals (*e.g.*, electron adducts to viologens, benzoate, nitrobenzene, acetophenone, nitrobenzoate, methylnicotinamide, and NAD^+) $k \sim 10^9 M^{-1}s^{-1}$. On the other hand, aliphatic radicals have lower k-values (*e.g.*, $CH_3\dot{C}OHCH_3$, 3.8 X 10^8; $^-O_2CCHOH\dot{C}OHCO_2^-$, 1.7 X 10^8; $CH_3\dot{C}OHCO_2^-$, 2.3 X 10^8; and $CH_2OH\dot{C}OHCH_2OH$, 2.5X10^6; all in $M^{-1}s^{-1}$), despite being good electron donors. These results indicate the high efficiency of π-π interactions in the reduction of cyt(III)c. Some k values change as the pH is increased above 7, *e.g.*, for O_2^-, k=1.6 X $10^6 M^{-1}s^{-1}$ at pH <7 while k=4 X 10^4 $M^{-1}s^{-1}$ at pH=10.4, presumably because the conformation of cyt(III)c changes with pH. The results indicate that several mechanisms for electron transfer are operative. The implications to electron transport system will be discussed.

F-AM-E7 PHYSICAL ASPECTS OF MEMBRANE PROTON UPTAKE AND UBIQUINONE REDUCTION. Katie M. Petty* and P. Leslie Dutton*, (Intr. by E. Mochan), Johnson Research Foundation, University of Pennsylvania, Philadelphia, Pa. 19174.

Factors governing the reactions leading to proton (H^+) uptake and release in photosynthetic membranes (chromatophores) from Rps. spheroides have been investigated using single and multiple single-turnover flash activation in combination with controlled redox potential, pH, temperature and viscosity. Optical assays of externally added indicator dyes were used to measure H^+ uptake. An electron is delivered to membrane ubiquinone (UQ) from the reaction center protein primary acceptor (photoredoxin; Pd) which is reduced (Pd^-; < 1 nsec) following a short flash. 1.0 ± 0.05 H^+ is uptaken per electron delivered to UQ. The t1/2 of H^+ uptake at pH 7.0 is 150 μs; the rate is indicator dye concentration insensitive. The apparent activation energy (E_A; 4-40°C) of the H^+ uptake is 10.5 Kcal/mole. The rates and E_A are not significantly affected by 50% ethylene glycol (∿x 10 increase in viscosity; 20°C). However, the fact that the rate of H^+ uptake increases less than 10 fold over the 5.3 to 8.3 pH range indicates that the protonation is not the rate limiting step in the UQ reduction/protonation reaction. Thus no rate limiting H^+ permeability barrier exists between the H^+ and reduced UQ, UQ being in effective contact with the external membrane/aqueous interface. Hence, the rate of H^+ uptake gives a measure of the rate of UQ reduction by the reaction center protein's Pd^-. Supported by PHS GM 12202 and NSF GB 28125.

F-AM-E8 DISTRIBUTION AND REACTIVITY OF THE IMMUNODETERMINANTS OF CYTOCHROME C OXIDASE ON THE INNER MITOCHONDRIAL MEMBRANE. Charles R. Hackenbrock and Katy Miller-Hammon,* Department of Cell Biology, University of Texas Southwestern Medical School, Dallas, Texas, 75235.

Purified IgG, specific for cytochrome c oxidase (cyt aa_3), has been prepared by affinity chromatography. Ouchterlony diffusion analysis shows a single precipitating band of IgG against cyt aa_3 and no precipitating band against cytochrome c. 200 μg of IgG completely inhibits State 3, 4, and 3U respiration in mitoplasts (2 mg protein) within 2-4 sec. Site specific binding of IgG to cyt aa_3 is indicated by inhibition of respiration in the presence of Antimycin, ascorbate and TMPD. IgG also completely inhibits the reduction of ferricyanide using succinate as the electron donor. The binding of ^{125}I-IgG to the immunodeterminants of cyt aa_3 displaces cytochrome c resulting in a loss of the 550 nm band but no change in the 604 or 562 nm bands of the mitoplast membrane. Sonicated vesicles prepared from mitoplasts show complete respiratory inhibition by IgG to cyt aa_3 in the presence of Antimycin, ascorbate and TMPD. Thus at least two respiratory-inhibiting antibodies occur in the affinity purified IgG; one to an immunodeterminant located close to the site of reduction and one located close to the site of oxidation. IgG was conjugated to ferritin for visual probing of the distribution of immunodeterminants of cyt aa_3 on the mitoplast membrane. The purified conjugate shows immuno-activity and respiratory inhibition activity identical to the unconjugated IgG. Immunodeterminants of cyt aa_3 are observed as close together as 400 Å on the outer surface of the inner membrane. Our results show that oxidase is diffusely distributed in both the cristal membrane and inner boundary membrane. (We thank Dr. Tsoo King for cyt aa_3; supported by NSF Grant Number BMS72-02372 A02).

F-AM-E9 THE EFFECT OF FREE FATTY ACID LEVELS ON THE OXIDATIVE PHOSPHORYLATION IN RAT LIVER MITOCHONDRIA. E. Higgins* and S.H.P. Chan, Department of Biology, Syracuse University, Syracuse, New York 13210.

Changes in the respiratory control index (RCI) and ADP/O ratio were found to be related to alterations in the free fatty acid levels of rat liver mitochondria aging in 0.25M sucrose, 10mM tris-Cl, 1mM EDTA buffer (STE) at 0°C. The free fatty acids were extracted with chloroform and determined by colorimetric methods and by gas liquid chromatography. Following isolation, free fatty acid levels increased with time while a concomitant decrease in the RCI and ADP/O ratio occurred. The changes of free fatty acid levels correspond to the reported increasing levels of phospholipase A activity in aged mitochondrial preparations. After 9-10 hours, the rate of free fatty acid production was accelerated with a corresponding faster rate of decrease in the RCI and ADP/O ratio. Washing this viable mitochondria (RCI>1) with STE containing 1% bovine serum albumin (BSA) produced a reverse aging effect on the RCI (e.g., 1.2 to 2.2) and free fatty acids (e.g., 16nmoles to 4.8 nmoles/mg protein). This reversible phenomenon remained possible until the mitochondrial activity is depleted (RCI=1). This study indicates a direct correlation between the level of endogenous fatty acids and the uncoupling of mitochondrial oxidative phosphorylation. Presently we are studying whether the free fatty acids are removed by the BSA washes or the BSA is incorporated into the mitochondria as a repair mechanism. This work is supported by a grant from the American Heart Association, Finger Lakes Chapter.

F-AM-E10 THE EFFECT OF LACTOPEROXIDASE-CATALYZED IODINATION ON THE INTEGRITY OF MITOCHONDRIAL MEMBRANES. C.T. Huber* and M. Morrison, Laboratory of Biochemistry, St. Jude Children's Research Hospital, Memphis, Tenn. 38101.

Incorporation of large amounts of iodide into mitochondria causes breakage of mitochondrial membranes. The release of adenylate kinase, a soluble enzyme in the intermembrane space, indicates that the outer membrane breaks after incorporation of 0.2 nmoles or more iodine atoms per mg of protein. The release of glutamic dehydrogenase, an enzyme located in the matrix space, and soluble protein suggests rupture of the inner membrane after still larger amounts of iodide are incorporated. After incorporation of 3.0 nmoles I/mg examination by the electron microscope reveals a change from the condensed to the swollen morphology. Lipid peroxides and I_2 are not intermediates in the disruptive effect of extensive lactoperoxidase-catalyzed iodination on the membranes. During iodination at pH 6.5 almost no release of glutamic dehydrogenase and protein is detectable and the loss of adenylate kinase from the particulate is diminished. The data indicate that lactoperoxidase-catalyzed iodination can be used as a probe of mitochondrial membrane surfaces as long as the amount of iodide incorporated is kept sufficiently low. (This work was supported in part by an Institutional grant, IN-99 from the American Cancer Society and a grant from NIH, CA 13534.)

F-AM-E11 DETERGENT INACTIVATION AND REACTIVATION OF MITOCHONDRIAL RESPIRATION. R.J. Mehlhorn and L. Packer, Membrane Bioenergetics Group, Energy and Environments Division, Lawrence Berkeley Laboratory, University of California, Berkeley, Ca. 94720.

Respiration of rat liver mitochondria can be inhibited by the cationic detergent CTAB (cetyl trimethyl ammonium bromide) and the anionic detergent SDS (sodium dodecyl sulfate) at the level of about 1 detergent molecule per phospholipid. Inhibition produced by either detergent can be reversed by adding ca. 1 equivalent of the detergent with opposite charge (J. McGuire collaboration). A unique feature of the reversible effect of the detergent inhibition-reactivation effects on respiration is the virtually immediate loss and recovery of activity. At higher concentrations of the inhibiting detergent, reactivation cannot be brought about by charge neutralization. However, mitochondria crosslinked with bifunctional imidoesters are stabilized such that higher detergent levels are required for both inactivation and reactivation (P. Chun collaboration). Spin labeling was used to correlate structural effects in the lipid domains with detergent induced loss and recovery of respiratory function. Light scattering and gel electrophoresis studies have been used to further characterize the detergent effects upon the membrane and its components.

F-AM-E12 LIGHT SCATTERING FROM SUBMITOCHONDRIAL PARTICLES. B. T. Storey, C. P. Lee*, S. Papa*, S. Rosen*, and G. Simon*. Depts. of Obstetrics and Gynecology, Biophysics and Physical Biochemistry, and Physiology, Univ. of Pennsylvania, Philadelphia, Pennsylvania 19174.

Membrane fragments prepared by sonication of beef heart mitochondria in the presence of EDTA (ESMP) show a 90° light-scattering decrease upon energization with succinate in the presence of salts, consistent with swelling of the particles (Papa et al. (1973) Biochem. Biophys. Res. Comm. 52, 1395). The intensity of light scattered from ESMP at 45° and 90° (I_{45} and I_{90}) is linear with particle protein concentration (C) to 1.6 mg protein/ml; at 135°, I_{135} is non-linear with C, but I_{135}/C is linear in C with a negative slope. The values of $Z = I_{45}/I_{135}$ extrapolated to C = 0 fall within the range of validity of the Rayleigh-Gans-Debye (RGD) theory for determining particle size by light scattering (Jennings & Jerrard (1965) J. Colloid Sci. 20, 448). The calculated diameter is 190 nm in sucrose solution, independent of sucrose concentration to 2.0 M; this value is consistent with the size range reported for ESMP by Huang et al. (1973) Biochim. Biophys. Acta 305, 455. Changes in light scattering from ESMP must therefore be due to change in particle dimension, and not to changes in particle refractive index (n_p). Values of I_{45}, I_{90}, and I_{135} all decrease with increasing sucrose concentration, equivalent to increasing solvent refractive index (n_s). They all extrapolate to zero at the point where $n_s = n_p$, giving $n_p = 1.444$ at 25°.

Supported by NSF GB-23063 and USPHS GM-19636.

F-AM-F1 SOLID-PHASE ISOLATION AND KINETIC CHARACTERIZATION OF MAMMALIAN MYOGLOBINS. J. LaGow and L. J. Parkhurst, Dept. of Chemistry, University of Nebraska, Lincoln, Nebraska 68508.

A new rapid preparation for mammalian myoglobins has been devised which utilizes a solid-phase mercurial resin. Previous methods involved fractionation by ammonium sulfate precipitation and gel filtration chromatography with G-75 or G-100 Sephadex, which, for large samples, requires a minimum of 10 hrs. This latter procedure results in significant met formation and is totally unsuited for micro-scale operation. The new method uses the mercurial resin to bind hemoglobin, which is the major heme contaminant in all mammalian preparations. Since the method relies on the difference in SH reactivity between hemoglobin and myoglobin rather than on molecular weight, a small column allows rapid separation and quantitative recovery of myoglobin and permits the isolation of myoglobin from as little as 200 mgs of muscle tissue. This method has been used for the isolation of myoglobins from human, dog, and beef skeletal and cardiac muscle in amounts sufficient for electrophoretic studies and measurements of ligand-binding kinetic and equilibrium constants. The ligand-binding kinetics and equilibria of the 3 myoglobins for the ligands CO, O_2, F^-, CN^-, and N_3^- have been studied by stopped-flow, and flash- and dye-laser photolysis. Our kinetic measurements on these myoglobins are the first to be reported. Of particular interest are the results for N_3^- binding which show that the rate constants for this ligand are very sensitive to amino acid differences among mammalian myoglobins. These N_3^- association constants are in the ratios: 6.2(beef):4.2(human):3.8(dog):2(horse):1 (whale). Similar sensitivity is not found in O_2 and CO kinetics. (This work was supported by: NIH Grant No. HL 15284-03, a Nebraska Heart Assoc. Grant-in-Aid, and the Cardiovascular Center, Univ. Neb. Med. Center.)

F-AM-F2 ASSOCIATION OF METHANOL AND ETHANOL WITH METMYOGLOBIN. Arthur S. Brill and Mary E. McKnight*, University of Virginia, Charlottesville, Virginia 22901 USA.

Equilibrium associations of methanol and ethanol with methemoglobin produce EPR and optical absorption spectral changes in the heme moiety. Since no such changes are observed for metmyoglobin, the possibility that methanol and ethanol associate with metmyoglobin was investigated by measuring the effect of these alcohols upon the binding of cyanide as determined by optical difference spectroscopy in the Soret and visible. In these experiments the distribution of species may be described by three independent equilibria characterized by the dissociation constants $K_1 \equiv$ [metMb][CN]/[metMb-CN], $K_2 \equiv$ [metMb-CN][ROH]/[metMb-CN-ROH] and $K_3 \equiv$ [metMb][ROH]/[metM-ROH]. K_1 is measured directly. Assuming that the metMb-cyanide and metMb-cyanide-alcohol complexes have the same absorptivity spectrum, one finds that the measured $K_{eff} \equiv$ [metMb][CN]/([metMb-CN-ROH] + [metMb-CN]) is related to the three equilibrium constants by $K_{eff} = K_1 (1+[ROH]/K_3)/(1+[ROH]/K_2)$ under appropriate experimental conditions. The data obtained for methanol up to 3M fit this relation well, yielding values for K_2 and K_3 of 4.7 and 0.13M respectively with K_1=5.0μM. The data do not support direct competitive binding. It thus appears that methanol forms an association complex with metmyoglobin, that the cyanide and alcohol binding sites are distinct, and that these two associations are thermodynamically linked. Experiments with ethanol, which must be kept at low concentration because of denaturing effects, show a similar but much smaller influence of this alcohol upon the binding of cyanide to metmyoglobin. (Supported by USPHS, Grant No. HL 13989, National Heart and Lung Institute.)

F-AM-F3 OPTICAL AND OXYGEN BINDING PROPERTIES OF SYNTHETIC GREEN FORMYLMYOGLOBINS. M. Sono* and T. Asakura
Department of Pediatrics and Biophysics, Children's Hospital of Philadelphia and University of Pennsylvania, Philadelphia, Pennsylvania, 19104.

Three kinds of green synthetic myoglobin were prepared by recombination of horse heart apomyoglobin with two isomers of monoformyl-monovinyl-, and 2,4-diformyldeuterohemins. The formylhemins were prepared by the permanganate oxidation of protoporphyrin(Biochemistry, 13, 4386, 1974). The oxygen affinities(P_{50}) of spirographis and 2,4-diformylmyoglobins are 2.7 and 2.8 mmHg, respectively, at 25°, and about 2.5 times lower than that of native protomyoglobin, while that of isospirographis myoglobin is 1.0 mmHg and is similar to native myoglobin. Spirographis oxymyoglobin has absorption maxima(α, β and Soret bands) at 601, 556.5 and 435 nm, isospirographis oxymyoglobin at 595, 550, 429 nm, and 2,4-diformyl oxymyoglobin at 603, 563.5 and 447 nm. The optical red shifts as well as the decrease in the oxygen affinities of these myoglobins are attributed mainly to the presence of strongly electron attractive formyl side chains. Since the free isomers of monoformyl-monovinylhemin have similar properties, the differences observed after recombination with apoprotein must be caused by interactions with apomyoglobins. The degree of such a protein effect may be estimated by comparing the absorption spectra of heme before and after recombination, and was found to differ among the various myoglobins. Comparison of the oxygen affinities of the myoglobins taking account of this protein factor showed that the increase in the P_{50} values are inversely related to that in the pK_3 values of the free porphyrins. These results suggest the involvement of π-bonding in determining the oxygen-iron bond strength.
Supported by NIH grants HL-14679, HL-16734 and NHLI-2962B. T. A. supported by NIH: 5-K04-GM47463.

F-AM-F4 APPLICATION OF THE TANFORD-KIRKWOOD THEORY TO HYDROGEN ION EQUILIBRIA IN MYOGLOBINS. S.J. Shire, G.I.H. Hanania and F.R.N. Gurd.
University of Connecticut, Storrs, Conn., 06268, American University of Beirut, Beirut, Lebanon and Indiana University, Bloomington, Indiana, 47401

A semi-empirical modification of the Tanford-Kirkwood theory involving the introduction of solvent accessibility parameters for the various ionizing groups has been applied to the computation of titration curves of the major and minor components of sperm whale ferrimyoglobin (Shire, Hanania and Gurd. 1974, Biochemistry 13,2967). The comparison of the computed curves with the experimentally determined curves yielded good agreement. We wish to report here an extension of the theory to the titration curves of ferrimyoglobin from the following animal species: horse, California grey whale, harbor seal and California sea lion. The coordinates and static solvent accessibility parameters used in the computations were estimated in terms of the sperm whale myoglobin structure and the known amino acid sequences of the different myoglobins. Hydrogen ion potentiometric titrations at 0.01 M ionic strength and 25° were determined for the myoglobins as well as the spectrophotometric determination of the ionic strength variation of the ionization pK value of the iron-bound water molecule. These experimentally determined data were compared with the computed results. Also, when possible experimentally determined ionization pK values of individual groups in the protein were compared to the computed values. Some interesting comparative features of charge and ionization properties among the various myoglobins are presented.

This research was supported by PHS Grant OHL 05556.

F-AM-F5 LOW FREQUENCY RESONANCE ENHANCED RAMAN BANDS OF HEMEPROTEINS: DEPENDENCE ON SPECIFIC LIGANDS AND PROTEIN ENVIRONMENT. L. Rimai and I. Salmeen, Sci. Res. Staff, Ford Motor Co., Dearborn, MI 48121. T. Yamamoto*, Div. Biol. Sci., Cornell Univ., Ithaca, N.Y. D. H. Petering*, Chem. Dept., Univ. Wisc.-Milwaukee, Milwaukee, Wisc. 53201.

Resonance enhanced Raman spectra of hemeproteins contain a number of vibrational transitions in the 100 to 600 cm^{-1} region which become particularly strong when the exciting wavelenth is near the Soret band. Whereas the vibrational modes above 600 cm^{-1} can be assigned to the conjugated macrocycle, a number of the bands below 600 cm^{-1} correspond to vibrations of the iron-pyrrole nitrogen complex. These modes should be influenced directly by the nature of the axial ligands, and, in principle, by the position and orientation of those amino acid residues that interact with these ligands. We have recorded the low frequency resonance Raman spectra, with 441.6 nm excitation, of hemoglobin and myoglobin derivatives, cytochromes c and b_5, horseradish peroxiduse, catalase and cytochrome c oxidase. These experimental results show definite features characteristic of spin and oxidation states, type of porphyrin, specific axial ligands and protein environment. Thus, this spectral region contains information important in establishing the usefulness of resonance Raman spectroscopy as a structural as well as analytical tool in hemeprotein studies.

F-AM-F6 INTERACTION OF THE HEME PROTEIN P-450 WITH SMALL LIGAND MOLECULES: A STUDY OF ITS COMPLEX FORMATION WITH NITRIC OXIDE. Heinz Schleyer, David Y. Cooper* and Otto Rosenthal.* Harrison Dept. Surg. Res. and Johnson Res. Fdn., School of Medicine, University of Pennsylvania, Philadelphia, Pa., 19104, U.S.A.

Nitric oxide (NO) binds strongly to heme proteins in both 3+ and 2+ valence states. As part of an extensive investigation of the interaction with small gaseous ligands, we have studied the binding of NO to P-450 from adrenal cortex (JBC 247,6103) employing optical absorption and EPR spectroscopy. Parallel experiments were performed with microsomal preparations from rat liver. P-450(Fe^{3+}) combines readily with NO but, unlike the situation with other heme proteins (JBC 247,2447), the obtained complex is paramagnetic (S=1/2) and contains the metal ion in a formal 2+ state, as shown by exchange of NO with ligands specific for the ferrous heme protein. No intermediate steps have been detected. The NO-complex can also be prepared by reaction of NO with P-450(Fe^{2+}). The optical absorption spectra are non-distinct, with poorly resolved maxima near 419 and 439 nm. EPR spectroscopy shows strong delocalization of the spin density from the paramagnetic ligand into the heme group. The resulting spectrum is anisotropic (g-tensor 2.017, 2.04, 2.102) and exhibits partially resolved ^{14}N-hyperfine splitting (a_1~17, a_3~24 Oe). Microsomal preparations yield essentially identical results. A study of the pH-dependence in the range pH 6-13 allows comparison with the corresponding NO-complexes of modified ferrous heme proteins. These complexes are discussed in relation to the native heme protein, and pathways for the mechanism of reduction upon combination with NO are suggested.
(Supported by Grant NIH, PHS 5R01 AM 04484 - 15).

F-AM-F7 EPR STUDIES OF MODEL COMPOUNDS FOR NITROSYL-HEME PROTEINS. Y. Henry*, J. Peisach and W. E. Blumberg, Albert Einstein College of Med., Bronx, N. Y. 10461 and Bell Labs., Murray Hill, N. J. 07974.

Nitrosyl hemoglobin A (HbNO) exhibits a 9-line superhyperfine (shf) in the EPR proving interaction of the unpaired spin of the NO with the nitrogen atom from the proximal imidazole. Dependent upon the spin state of the β-chains or the presence of effectors such as H^+ or IHP, the protein undergoes a transition which is characterized by a change of shf pattern from 9 to 3 lines. In order to understand the nature of this transition, heme-NO complexes with various p-substituted anilines and pyridines as counter ligands were studied using EPR. Two types of spectra were observed. With electron withdrawing p-substituents (e.g. -CN), only interaction with the N of NO could be seen (3-line shf, A_{N1} = 16 gauss) at g_z = 2.009. With electron supplying substituents, (e.g. $-CH_3$), interaction with both axial N's was observed (9-line shf, A_{N1} = 21 gauss, A_{N2} = 6.5 gauss) at g_z = 2.005. Thus, contribution of pi-electron density from the counter ligand is correlated with an increased interaction between the electron spin of the NO and the nuclear spin of the counter ligand nitrogen. In addition, there is decreased interaction between the electron spin and the nuclear spin of the NO, increasing A_{N1}. It is believed that for the 3-line spectrum, the unpaired spin from the NO lies in the $3d\pi$ orbital of the NO moiety, while for the 9-line case there is transfer of the unpaired spin to an e_g orbital of the iron atom. This analysis suggests that when a 9-line shf pattern is observed for a nitrosyl hemoprotein, the contribution of pi-electron density by the proximal ligand to the iron is greater than when a 3-line shf pattern is observed for the same protein. For HbNO, it is suggested that the type of EPR observed depends upon the state of protonation of nitrogen N-3 of the proximal imidazole.

F-AM-F8 OPTICAL ACTIVITY OF HEME-c PEPTIDE SYSTEMS. A. Pande*, Lawrence H. Macdonald*, and Yash P. Myer, Department of Chemistry, State University of New York at Albany, Albany, New York 12222

Heme octapeptide, heme undecapeptide, cytochrome c heme fragment with 65 amino acids and cytochrome c under conditions resulting in symmetrical axial coordination configuration of the heme group, i.e. identical ligand field groups irrespective of their nature and/or ligand field strengths, results in complete loss of optical activity of the Soret π-π^* transition+ in other parts of the visible spectrum. In situations when one of the two axial positions is occupied by imidazole of histidine residue adjacent to the heme-bonded cysteine side chain and the second by either a low-ligand field group or a high ligand field group, all exhibit almost symmetrical positive Soret dichroic band with ellipticities varying from 3.5 to 11 x 10^4 deg.cm^2/ decimole of heme. The height of the Soret ellipticity band when compared to the difference in the ligand field strengths of the two axial ligands exhibits a relationship suggesting that the rotatory strength is proportional to the difference of ligand field strengths of the axially liganded functional groups. Interpretation of these observations seems to rest in the idea that the origin of the activity in heme transitions lies in the low symmetry of the heme group resulting because of the axially liganded groups rather than the transition dipole coupling mechanism operational in nonheme c systems.

F-AM-F9 UNFOLDING KINETICS OF CYTOCHROME C BY A SMALL PRESSURE PERTURBATION METHOD*, T. Bruckman*, E. L. Elson* and B. W. Maxfield (intr. by R. K. Clayton) Department of Chemistry, Cornell University, Ithaca, New York 14853.

The kinetics of folding and unfolding of cytochrome C are being studied using a new pressure perturbation technique which induces minimal departures from conformational equilibrium. Reaction progress is indicated by visible light absorbance by the heme group. A single pressure change of 3 atmospheres induces an absorbance change of from 10^{-3} to 10^{-4} of the change resulting from the complete unfolding of the native enzyme. Signal averaging of repetitive perturbations is necessary to obtain precise kinetic information. Characteristic amplitudes and relaxation times, τ, in the millisecond range have been measured as a function of temperature and pH. At pH = 2.0 (20mM $NaClO_4$ + $HClO_4$), τ decreases with increasing temperature while the amplitude increases to a maximum in the region of maximum slope in the equilibrium curve. At pH = 2.5 the behavior is significantly different and between pH = 3 and 4 no relaxation effects could be observed. Insofar as experimental conditions are comparable, our results agree with those previously obtained by other methods (eg. T. Y. Tsong, Biochemistry, 12, 2209 (1973)). One simple interpretation attributes the pH dependence of the amplitude to differences in the volumes of the unfolded and folded forms of the protein caused by carboxyl ionization. Studies of faster and slower components of the conformational transition and salt effects are underway. Kinetic decomposition of the pressure induced folding should provide valuable information about the mechanism of the process.

*Supported by NIH grant GM16927.

F-AM-F10 COMPARISON OF HYDRODYNAMIC STRUCTURE WITH ACTUAL STRUCTURE FOR HELIX POMATIA HEMOCYANIN. A. Kent Wright, Biochemistry Department, University of Tennessee, Center for Health Sciences, Memphis, Tennessee 38163, and Wayne W. Fish,* Biochemistry Department, Medical University of South Carolina, Charleston, South Carolina 29401.

An equivalent ellipsoid of revolution has been calculated for Helix pomatia hemocyanin in aqueous solvent. This model is a prolate ellipsoid with semi-major and minor axes of 681 and 135 A°, respectively, which is in agreement with hydrodynamic data based on transient electric birefringence, viscosity, and sedimentation velocity. This model is also compared with the structural model, a right circular cylinder of length 396 A° and 406 A° diameter, resulting from electron microscopy and three dimensional image reconstruction. The translational friction coefficient for the structural model, calculated according to Kirkwood's theory, agrees with that for the equivalent ellipsoid. The expected low angle X-ray scattering for the structural model is in agreement with observed scattering.

F-AM-F11 EXTENDED X-RAY ABSORPTION FINE STRUCTURE OF IRON IN SOLUTIONS OF HEMES AND HEME PROTEINS.

R. G. Shulman, P. Eisenberger*, W. E. Blumberg and S. Ogawa, Bell Laboratories, Murray Hill, N.J. 07974, and S. Doniach* and B. Kincaid*, Stanford Synchrotron Radiation Project+, Stanford, Ca. 94305.

The high photon flux of monochromatic x-rays available at the Stanford Synchrotron Radiation Project allows one to measure x-ray absorption, near the K edge of iron, in dilute iron compounds. We have obtained x-ray absorption spectra with resolved fine structure from iron compounds as well as from hemes and heme proteins in solution. The absorption at energies up to the edge includes several sharp excitonic bands, which along with the edge, depend upon the electronic properties of the iron and its neighbors. For example the edge is ~6 electron volts higher in FeF_3 than in FeF_2 while in ferri-hexacyanide it is only $1\frac{1}{2}$ electron volts higher than in ferro-hexacyanide. Solutions of horse heart cytochrome c at pH 7 showed an edge shift of 1 volt to lower energies upon reduction with ascorbate, while the ferric form shifted 3 electron volts to higher energy at pH 10.5. Hence changing the sixth ligand from methionine to lysine shifts the edge more than a change in formal charge. Comparisons have also been made of edge energies in solution of bis imidazole iron III protoporphyrin IX, oxy and deoxy hemoglobin and met myoglobin. Structural information in the neighborhood of the iron comes from the interference patterns observed at energies above the band edge. This information can be obtained from solutions as well as crystals.

+Supported by the NSF in collaboration with Stanford Linear Accelerator Center.

F-AM-G1 INTERACTION OF TOBACCO MOSAIC VIRUS PROTEIN (TMVP) WITH BOVINE SERUM ALBUMIN (BSA). Ragaa A. Shalaby and Max A. Lauffer, Department of Biophysics and Microbiology, University of Pittsburgh, Pittsburgh, Pennsylvania 15260.

It has been known for approximately three decades that tobacco mosaic virus (TMV) can be precipitated by BSA and by hydrophobic substances such as heparin even when the virus and the precipitant both have negative charges. Many reports have since appeared on the interaction of macromolecules with each other and with viruses and proteins. In the present study, the effect of several concentrations of BSA on the reversible entropy-driven polymerization of TMVP was followed by turbidity measurements. The effect of BSA depends upon its concentration and upon pH and ionic strength. In general, BSA promotes TMVP polymerization, i.e, causes it to occur at lower temperatures, and this effect increases with increasing BSA concentration. The pH dependence is illustrated by the finding that in 0.1 μ phosphate buffer, the effect of 6.7% BSA at pH 6.0 is about the same as that of 4% BSA at pH 6.5 and is approximately a 4° shift to lower polymerization temperatures. A concentration of 6.7% BSA at pH 6.5, however, leads to denaturation on increasing the temperature. Even though increasing ionic strength promotes polymerization of TMVP in the absence of BSA, the effect of increasing ionic strength from 0.10 to 0.18 decreases the polymerization promoting effect of BSA. While the ionic strengths involved are in the "salting out" range for TMVP, they are in the "salting in" range for many proteins. A formal description of the phenomenon, similar for all of the interactions mentioned, is that the activity coefficients of BSA and of TMVP are each increased by increasing the concentration of the other.

F-AM-G2 NOVOBIOCIN-BOVINE SERUM ALBUMIN COMPLEX. Joseph G. Brand* and Taft Y. Toribara* (Intr. by Isaac Feldman), Department of Radiation Biology and Biophysics, University of Rochester, Rochester, New York 14642.

The complex formed by the association between the drug, Novobiocin sodium, and bovine serum albumin (BSA) has been studied using the techniques of equilibrium dialysis and circular dichroism (CD). Equilibrium dialysis measurements made on the complex at 4°, 30° and 38° and analyzed by the Scatchard plot give evidence for heterogeneity of binding. The plots are non-linear, and the extent of their non-linearity is temperature dependent. These results indicate that there may be from 5 to 7 binding sites on BSA for Novobiocin that are of relatively high affinity as well as an undetermined number of low affinity sites.

Circular dichroic studies performed with the asymmetric drug complexed with BSA show that the drug's CD is perturbed upon binding. This perturbation is used in conjunction with a computer assisted least squares fit of the dialysis data to a three constant equation to generate these constants for the heterogeneous Novobiocin sites on BSA. Both the CD and the equilibrium dialysis data give evidence for a unique high affinity site ($n_1 = 1.0$) with $\Delta F_1^\circ = -7.03$ kcal. at 30°. Additional sites that cause CD perturbations of the drug can fit models with $n_2 = 5$ or 6. It is unclear as to which of these two models is the most appropriate.

This work was supported, in part, by a USPHS Grant No. DE-00175 and in part by the United States Atomic Energy Commission, Contract No. AT(30-1-)-49 and has been assigned Report No. UR-3490-642.

Biophysical Journal vol. 15, 1975 **290a**

F-AM-G3 LASER FLASH PHOTOLYSIS STUDY OF TRIPLETS OF POLYCYCLIC AROMATIC MOLECULAR PROBES COMPLEXED WITH SERUM ALBUMINS. T.J. Flamer, T. Prusik, J.M. Khosrofian* and N.E. Geacintov. Chemistry Department, New York University, New York, N.Y. 10003.

The transient triplet-triplet absorption spectra of various polycyclic aromatic molecules physically complexed to bovine serum albumin (BSA) and human serum albumin (HSA) dissolved in water have been obtained using conventional and laser flash photolysis techniques. In deaerated solutions of 3,4 benzopyrene complexed to BSA, triplet lifetimes as long as 65 milliseconds have been observed at 24°C.

The triplet molecules are readily quenched by oxygen in air saturated solutions yielding lifetimes varying from 15-40 microseconds for pyrene, 1,2 benzopyrene, 3,4 benzopyrene, 1,2 benzanthracene, 7,12 dimethylbenzanthracene, acridine orange and 1-anilino-8-naphthalene sulfonic acid. For example, the Stern-Volmer quenching constant for the triplet of pyrene in BSA is 9×10^7 M^{-1} s^{-1} while that of the singlet, determined by single photon counting, is 1.5×10^9 M^{-1} s^{-1}. The difference in the singlet and triplet quenching constants (by a factor of 15) is attributed to a combination of spin-selection rules and Franck-Condon factors in the quenching process of triplets by molecular oxygen. The quenching constant of the singlet of pyrene in water is 10^{10} M^{-1} s^{-1}, seven times larger than in BSA.

The oxygen quenching constant of the triplets varies by a factor of 10-15 in the temperature range of 10-40°C. This effect cannot be accounted for by changes in intrinsic viscosity and the diffusion of oxygen in water and is probably due to conformational changes in the protein.

The triplet state is a sensitive probe of the oxygen concentration in its microenvironment which is useful in photodynamic studies. This work is funded by Public Health Research Grant CA14980 of National Cancer Inst.

F-AM-G4 ^{13}C SPIN LATTICE RELAXATION TIMES TO STUDY THE INTERACTION OF SUCROSE AND MELEZITOSE WITH CONCANAVALIN A. Joseph J. Villafranca and Ronald E. Viola,* Department of Chemistry, The Pennsylvania State University, University Park, Pennsylvania 16802

The spin lattice relaxation rates ($1/T_1$) of the natural abundance ^{13}C of all 12 carbons of sucrose (α-D-glucopyranosyl-β-D-fructofuranoside) were measured in the presence of Mn(II)-con A and Zn(II)-con A. Sucrose is a disaccharide which binds to con A and inhibits the dextran precipitation assay. The paramagnetic contribution to the relaxation rates was used to calculate the distance between the Mn(II) site and the disaccharide binding site. Using a correlation time of 30nsec for the rotational reorientation time of the protein dimer complex (Yang et al., J. Biol. Chem. 249, 7018 (1974)) the results are consistent with the binding of sucrose in a unique configuration on the surface of the protein. Both the glucosyl and fructosyl rings are 10-14 Å from the Mn(II). Distances were also measured to several carbons of melezitose (a trisaccharide) and a comparison is made between the binding of mono-, di- and trisaccharides on con A. This work was supported by NIH Grant A16661.

F-AM-G5 SALT DEPENDENCE OF fd GENE 5 PROTEIN DIMER FORMATION. PROPERTIES OF TYROSYL AND THIOL GROUPS IN MONOMERS, DIMERS, AND DNA-PROTEIN COMPLEXES.

H.T. Pretorius*, M. Klein*, and L.A. Day, The Public Health Research Institute of the City of New York, 455 First Ave., New York, N.Y. 10016

Equilibrium sedimentation has shown that gene 5 protein of fd bacteriophage is predominantly a dimer in neutral aqueous buffers near 0.2 M ionic strength. Monomers are obtained when the ionic strength is increased, and higher aggregates tend to form when it is decreased. The spectral properties (UV absorbance, CD, tyrosine fluorescence) of monomers and dimers are essentially the same. The different effects of NaF, NaCl, and $NaClO_4$ on the monomer-dimer equilibrium and on DNA binding have been examined.

Complexes of single-stranded fd DNA and gene 5 protein have been isolated from cell lysates (in vivo complexes), and also prepared by mixing isolated components (in vitro complexes). In vivo complexes, as isolated, contained from 900 to 1300 subunits of protein (9830 daltons each) per DNA molecule (5740 nucleotides), whereas in vitro complexes usually contained close to 1450 subunits per DNA. The two types of complex have similar spectral characteristics, including UV absorbance, CD, and strongly quenched tyrosine fluorescence, after account has been made for different relative amounts of protein and DNA present. It was also found that the single thiol group of each subunit in the complexes reacts slowly with 5,5'-dithiobis (2-nitrobenzoic acid) as was found for isolated protein monomers and dimers. The thiol group reacts rapidly in 6 M guanidine hydrochloride. Therefore, neither in vivo nor in vitro complexes contain disulfide bonds.

F-AM-G6 THE PARTIAL VOLUME SPECTRUM OF GUANIDINIUM CHLORIDE IN PROTEIN SOLUTIONS.

T. H. Crouch* and D. W. Kupke, Department of Biochemistry, School of Medicine, University of Virginia, Charlottesville, Va. 22901.

The partial volume changes, $\Delta\bar{v}$, of the components in a solution upon varying the composition provide considerably more information and insight than do the total volume changes, ΔV. Heretofore, it has been inconvenient to determine little more than gross changes in the apparent specific volumes of one of the components, usually the macromolecule; the perturbant (e.g., a denaturant) and water, however, may undergo greater changes in $\bar{v}$. Since compositions can be altered serially in microgram increments in the magnetic densimeter, we have determined the partial volume spectrum of guanidinium chloride (GCl) in ribonuclease-water solutions over the range 0 to 6 molar in GCl. Differences in $\bar{v}$(GCl) as great as 0.05 ml/g were observed when the protein was present. It was also feasible to determine $\Delta\bar{v}(H_2O)$ and $\Delta\bar{v}$(protein) at intervals along this partial volume curve. In addition, ΔV of mixing could be determined conveniently by density at various compositions, and these values were compared with those obtained from the partial volume data. Contrary to expectations, $\bar{v}$(protein) *increased* with GCl concentration; the value decreased, however, when β-mercaptoethanol was inserted into the medium.

(Supported by Grant, GB-27331, from the U. S. National Sci. Foundation.)

F-AM-G7 EXTENDED X-RAY ABSORPTION FINE STRUCTURE ANALYSIS. A NEW PROBE OF CHEMICAL AND ELECTRONIC STRUCTURE OF COPPER PROTEINS.

W.E. Blumberg and P. Eisenberger*, Bell Laboratories, Murray Hill, N.J. 07974, and S. Doniach* and B. Kincaid*, Stanford Synchrotron Radiation Project+, Stanford, Ca. 94305.

The location of the absorption edge of the K electrons from the copper atoms in copper complexes and copper proteins provides a sensitive indicator of the donation of electronic charge from the ligand atoms to the copper atom. Although the metal atom is formally dipositive, the absorption edge of cupric atoms shows that the local charge decreases to that of the metallic state and even beyond as the charge-donating abilities of the ligand atoms are changed. Nitrogen ligands donate more charge than oxygen atoms, and the greater the negative charge on the ligand atoms, the more negative charge becomes localized on the metal atom. A good correlation with the EPR-derived charge properties is obtained. In addition, there are excitonic features both below and above the absorption edge, which are indicative of Frankel excitons (Rydberg states) within the metal atom and of charge-transfer excitations involving the ligand atoms. These excitonic features may provide useful signatures for the chemical and electronic structure surrounding the metal atom. Beyond the absorption edge, interference features are observed which may be related to the interatomic distances of the metal-ligand complex via a Fourier analysis of the absorption spectra. Preliminary analyses of the extended fine structure features show that at least the first coordination sphere of ligand atoms and possibly further shells may be discerned. Studies of absorption fine structure features in copper proteins is underway and should prove useful in assigning structure and electronic state in unknown cases.

+Supported by the NSF in collaboration with Stanford Linear Accelerator Center.

F-AM-G8 MECHANISMS OF LENGTH DETERMINATION IN LINEAR PROTEIN AGGREGATES.

Victor A. Bloomfield and Terry Wagenknecht*, Department of Biochemistry, University of Minnesota, St. Paul, MN 55101.

Tails of bacteriophages such as T4 and λ, and many other linear or helical arrays of proteins, show striking constancy of length. The mechanism of length determination in these structures is not known, but two hypotheses enjoy current favor: a length determining factor (LDF) such as TMV-RNA, and Kellenberger's accumulated strain (AS) model. We have examined by statistical thermodynamics the consequences of these two hypotheses, to see what experiments might distinguish between them. The major conclusions are (1) Both models can predict suitably narrow length distributions with plausible values of the thermodynamic parameters. (2) The LDF model exhibits highly cooperative behavior, with either fully polymerized or very short aggregates being observed as the product KC of association constant and free monomer concentration is varied. Species of intermediate length will be observable only if the LDF is shortened. (3) If KC is lowered at constant AS free energy/monomer, shorter aggregates will be observed; but increasing KC will not yield longer polymers. As KC is lowered, the distribution will remain narrow.

F-AM-G9 KINETICS OF TOBACCO MOSAIC VIRUS PROTEIN (TMVP) SELF-ASSOCIATION. T. M. Schuster and R. B. Scheele, Biological Sciences Group, University of Connecticut, Storrs, CT 06268.

The association-dissociation reactions of TMVP exhibit unusual kinetics properties which can result in long-lived, metastable, virus-shaped, helical rods. Such overshoot in polymerization arises from the following kinetics properties. Polymerization occurs by a slow nucleation reaction (formation of 20S "disk protein") followed by a much more rapid elongation reaction (addition of a component of the 4S "A-protein"). Under conditions of low initial concentration of 20S nuclei (pH 6.5; temperature changed from 4° to 20°C in <3 min) this sequence of reactions can lead to an overshoot in polymerization when the rate of depolymerization of the non-equilibrium helical rods to the equilibrium molecular weight distribution is slow, as is the case below pH 6.6. The rate of depolymerization is pH-dependent and is reflected in the acid-base titration of the protein as a reproducible hysteresis loop, the magnitude of which at pH 6.2 corresponds to more than 50% of the polymerization-linked protons bound in the the equilibrium polymerized state. Ultracentrifuge measurements during slow depolymerization show that the helical rods dissociate to the equilibrium state by formation of 4S protein which then re-equilibrates to 20-25S and ca. 35S protein (disks and short, helical rods), near pH 6.5.

Supported by NIH grants GM-18472 and AI-11573.

F-AM-G10 RATE CONSTANTS FOR THE REVERSIBLE ASSOCIATION OF E. COLI RIBOSOMAL SUBUNITS. J.B. Chaires*, C. Ke*, M-S. Tai*, and G. Kegeles, Section of Biochemistry and Biophysics, University of Connecticut, Storrs, CT, 06268; A.A. Infante*, B. Kosiba*, and T. Coker*, Dept. of Biology, Wesleyan University, Middletown, CT, 06457.

Using a newly developed pressure-jump light scattering apparatus, we have determined the forward and reverse rate constants for the reversible association of E. Coli ribosomal subunits:

$$30S + 50S \underset{k''}{\overset{k'}{\rightleftharpoons}} 70S$$

A forward rate constant, k', of 21.5 $(g/dl)^{-1}sec^{-1}$, and a reverse rate constant, k", of 5.1 sec^{-1} have been observed at 20.5°C in a buffer consisting of 10mM Tris-HCl, 10mM Mg++, and 60mM KCl, pH 7.75. The association equilibrium constant is calculated to be $K(assoc.) = k'/k'' = 4.2(g/dl)^{-1}$. This implies that, under our conditions, association into 70S ribosomes is strongly favored. To check for the possibility of a reaction faster than the resolution time of our pressure-jump apparatus, temperature-jump light scattering experiments have been performed. A reaction of the order of 1 msec has in fact been observed, indicating that the association process may involve two discrete steps. These kinetic experiments provide quantitative confirmation of previous indications of a rapid equilibrium between the ribosome and its subunits.

Biophysical Journal vol. 15, 1975 294a

F-AM-G11 PHYSICAL PROPERTIES OF HEMOGLOBINS SPECIFICALLY CARBAMYLATED AT THE α- AND β-CHAIN AMINO TERMINI. R.C. Williams, Jr., Department of Biology, Yale University, New Haven, CT., L.L. Chung* and T.M. Schuster, Biological Sciences Group, University of Connecticut, Storrs, CT.

Human hemoglobins A and S, specifically carbamylated at the α- and β-chain valine amino termini were prepared by a simple chromatographic method (R.C. Williams, Jr., L.L. Chung and T.M. Schuster, Biochem. Biophys. Res. Comm., in press) that exploits the preferential binding of inositol hexaphosphate to the β-chain amino termini. These derivatives are of particular interest because the amino terminal groups have been implicated in the oxygen-linked binding to hemoglobin of CO_2, organic phosphates and H^+. Measurements of tetramer-dimer dissociation constants of the two doubly carbamylated derivatives ($\alpha_2^C\beta_2$ and $\alpha_2\beta_2^C$) and of the fully carbamylated derivative ($\alpha_2^C\beta_2^C$) were carried out by equilibrium ultracentrifugation, with the following results for CO-hemoglobin A (in 0.1 M NaCl + 0.05 M Tris + 0.001 M EDTA, pH 7.0, at 20.0°):

$\alpha_2\beta_2$: $K_{4,2}$ = 2.8 uM heme; $\alpha_2^C\beta_2$: $K_{4,2}$ = 0.29 uM heme

$\alpha_2\beta_2^C$: $K_{4,2}$ = 3.0 uM heme; $\alpha_2^C\beta_2^C$: $K_{4,2}$ = 0.28 uM heme

Since the tetramer-dimer dissociation constant of hemoglobin is a sensitive indicator of changes in its protein structure, these results are interpreted to indicate that significant conformational alteration is produced by carbamylation of the α-chain, while little or no such alteration is produced by carbamylation of the β-chain. Other properties of these derivatives are under study and will be reported. (Supported by Grants HL 12901, GM 18472 and AI 11573 of the National Institutes of Health.)

F-AM-G12 PROTEIN SEQUENCE RELATIONSHIPS FROM AMINO ACID COMPOSITIONS R. E. Dayhoff, L. T. Hunt*, and M. O. Dayhoff, Nat. Biomedical Res. Fdn., Georgetown Univ. Med. Cen., 3900 Reservoir Road, Washington, D. C. 20007

It is useful to estimate the probability of relationship of two proteins from their amino acid compositions. Such a measure can be applied before the sequence is available, and even afterwards it contributes a probability factor independent of the one based on scores of real and scrambled sequences. We have investigated a number of methods, using the average compositions of 119 families of proteins, which include 72 pairs known to be distantly related. First a simple comparison function, involving the percent composition f_i of each amino acid in the two families, was used:

$$\text{Composition scores} = \sum_{i=1,20} (f_i - f'_i)^2$$

Results were compared with scores that weighted the different amino acids according to their mutability and to scores that considered the cross terms between amino acids, weighting each pair by similarity. The more complex methods permitted better resolution of real relationships. The meaning of the scores in terms of probability is length dependent. It is also composition dependent; proteins with nearly average composition, such as glutamate dehydrogenase or the immunoglobulins, are similar to many more families than proteins of unusual composition, such as keratin or parvalbumin. Very distantly related model sequences were prepared by the accumulation of many point mutations. These gave more low scores than real sequences, reflecting additional processes in the evolution of proteins, such as the acceptance of many local duplications of genetic material propagating the necessarily unusual composition of a short region. *This work was supported by NIH Grant GM-08710 and NASA Contract NASW-2730.*

F-AM-G13 ELECTRON MICROTEPHROSCOPY OF PROTEINS: IMAGES OF MYOKINASE AND PROTAMINE WITH DETAIL AT 5-10Å. F.P. Ottensmeyer, R.F. Whiting*, E.E. Schmidt*, and R.S. Clemens*, Ontario Cancer Institute, 500 Sherbourne St., Toronto, Ontario, Canada M4X 1K9.

The enormous radiation doses required to obtain electron micrographs at high resolution of rather fragile biological specimens have fostered a rather pessimistic outlook on obtaining fine structural information at or below 20-25 Å. Contrast agents required in bright field microscopy on the one hand help to preserve the fine-structural arrangement, on the other hand hinder the attainment of resolution better than about 20 Å by their own coarse granularity. Dark field electron microscopy obviates the need for extraneous contrast agents and so removes this obstacle to higher resolution. Now however the unprotected biological specimen is completely subject to the untrammelled effects of electron irradiation. The high degree of destruction expected suggests that one is engaged in tephroscopy, or looking only at the ashes of the specimen. It remained to determine however how well details in the images of molecules so irradiated correspond to biologically meaningful structure. For one such molecule, myokinase (M.W. 22,000) we have been able to establish a correlation with the X-ray determined structure that indicates that detail well below 10 Å is still meaningful. Moreover, reproducible images of herring protamine (M.W. 5,000) suggest that with care a 5 Å resolution can be achieved.

F-AM-G14 SECONDARY STRUCTURES OF COAT PROTEIN AND DNA IN FILAMENTOUS BACTERIAL VIRUSES BY LASER-RAMAN SPECTROSCOPY. G.J. Thomas, Jr. and P. Murphy*, Department of Chemistry, Southeastern Massachusetts University, North Dartmouth, Massachusetts 02747.

Laser-Raman spectroscopy is a sensitive method for detecting different types of secondary structure in proteins and nucleic acids. The technique may also be used to investigate protein-nucleic acid interactions in viruses. We have undertaken a study of the filamentous bacterial viruses, Pf1 and fd, to determine the backbone conformations of viral DNA and coat protein subunits and to test molecular models proposed on the basis of X-ray diffraction data. Raman spectra of Pf1 and fd virions, the first obtained on true DNA-protein complexes, are unusual for their rich patterns of Raman lines and high signal-to-noise quality. Of the fifty or more frequencies detected for each virus, the vast majority are assignable to vibrations of the coat protein molecules. The different amino-acid compositions of Pf1 and fd coat proteins are easily recognized by their different side-chain vibrational frequencies. However the conformationally sensitive amide frequencies are identical for both viruses and indicate identical α-helical secondary structures. The Raman spectra also show that viral DNA backbones are not in a conformation of the A-type. The geometry of coat protein helices in either virus changes reversibly over the temperature range 0-75°C indicating considerable flexibility in the filamentous structure. The secondary structure of viral DNA appears quite stable, however, over the same temperature range.

Supported by NSF Grant GB 41382, NIH Grant AI-11855-01, and the Research Corporation.